INFORMATION TO USERS

This material was produced from a microfilm copy of the original document. While the most advanced technological means to photograph and reproduce this document have been used, the quality is heavily dependent upon the quality of the original submitted.

The following explanation of techniques is provided to help you understand markings or patterns which may appear on this reproduction.

1. The sign or "target" for pages apparently lacking from the document photographed is "Missing Page(s)". If it was possible to obtain the missing page(s) or section, they are spliced into the film along with adjacent pages. This may have necessitated cutting thru an image and duplicating adjacent pages to insure you complete continuity.

2. When an image on the film is obliterated with a large round black mark, it is an indication that the photographer suspected that the copy may have moved during exposure and thus cause a blurred image. You will find a good image of the page in the adjacent frame.

3. When a map, drawing or chart, etc., was part of the material being photographed the photographer followed a definite method in "sectioning" the material. It is customary to begin photoing at the upper left hand corner of a large sheet and to continue photoing from left to right in equal sections with a small overlap. If necessary, sectioning is continued again — beginning below the first row and continuing on until complete.

4. The majority of users indicate that the textual content is of greatest value, however, a somewhat higher quality reproduction could be made from "photographs" if essential to the understanding of the dissertation. Silver prints of "photographs" may be ordered at additional charge by writing the Order Department, giving the catalog number, title, author and specific pages you wish reproduced.

5. PLEASE NOTE: Some pages may have indistinct print. Filmed as received.

University Microfilms International
300 North Zeeb Road
Ann Arbor, Michigan 48106 USA
St. John's Road, Tyler's Green
High Wycombe, Bucks, England HP10 8HR

77-11,248

LOCKE, Douglas Peter, 1949-
He^3-VACANCY BOUND STATES, BOSE-EINSTEIN CONDENSATION, AND THE J PROBLEM IN SOLID He^4.

The University of Arizona, Ph.D., 1976
Physics, solid state

Xerox University Microfilms, Ann Arbor, Michigan 48106

He^3-VACANCY BOUND STATES, BOSE-EINSTEIN CONDENSATION, AND THE J PROBLEM IN SOLID He^4

by

Douglas Peter Locke

A Dissertation Submitted to the Faculty of the

DEPARTMENT OF PHYSICS

In Partial Fulfillment of the Requirements
For the Degree of

DOCTOR OF PHILOSOPHY

In the Graduate College

THE UNIVERSITY OF ARIZONA

1 9 7 6

THE UNIVERSITY OF ARIZONA

GRADUATE COLLEGE

I hereby recommend that this dissertation prepared under my direction by Douglas Peter Locke

entitled He^3-Vacancy Bound States, Bose-Einstein Condensation, and the J Problem in Solid He^4

be accepted as fulfilling the dissertation requirement of the degree of Doctor of Philosophy

Richard A. Mowrey — Nov 19, 1976
Dissertation Director — Date

After inspection of the final copy of the dissertation, the following members of the Final Examination Committee concur in its approval and recommend its acceptance:*

R. A. Mowrey	Nov. 19, 1976
John O. Stoner, Jr.	19 Nov. 1976
Donald R. Huffman	Nov. 22, 1976
Gerald K. Wangsness	22 Nov 1976
Robert H. Parmenter	23 Nov. 1976

*This approval and acceptance is contingent on the candidate's adequate performance and defense of this dissertation at the final oral examination. The inclusion of this sheet bound into the library copy of the dissertation is evidence of satisfactory performance at the final examination.

STATEMENT BY AUTHOR

This dissertation has been submitted in partial fulfillment of requirements for an advanced degree at The University of Arizona and is deposited in the University Library to be made available to borrowers under rules of the Library.

Brief quotations from this dissertation are allowable without special permission, provided that accurate acknowledgment of source is made. Requests for permission for extended quotation from or reproduction of this manuscript in whole or in part may be granted by the head of the major department or the Dean of the Graduate College when in his judgment the proposed use of the material is in the interests of scholarship. In all other instances, however, permission must be obtained from the author.

SIGNED: Douglas P Locke

ACKNOWLEDGMENTS

I would like to express my gratitude to my dissertation advisors, Dr. Richard Young and Dr. Allan Widom. Dr. Young's guidance and encouragement have been invaluable, especially under the difficult circumstance of completion of this work by correspondence. In addition to his regular professorial duties at Northeastern University, Dr. Widom kindly agreed to guide the research which makes up the third and fourth chapters of this work.

TABLE OF CONTENTS

TABLE OF CONTENTS--Continued

LIST OF ILLUSTRATIONS

LIST OF ILLUSTRATIONS--Continued

LIST OF TABLES

ABSTRACT

The existence of bound states and scattering resonances for both a He^3-vacancy system and a He^3-He^3 system in crystalline He^4 is demonstrated. For realistic physical parameters the theory yields binding energies corresponding to ~ 0.1 °K for the He^3-vacancy system and $\sim 10^{-4}$ °K for the He^3-He^3 system.

The He^3-vacancy bound states can have a profound effect on the diffusion of He^3 atoms because of the "fast" motion of these "molecules." This effect is discussed and compared with experiment. The existence of these "molecules" is indicated but not definitely established.

There has been considerable speculation about the possibility that solid He^4 can exist in a Bose condensed state closely analogous to the ordered state of superfluid He^4. Extending the arguments of Chester, Penrose and Onsager, quantitative predictions are made of the λ-anomaly in the solid phase. At a pressure of ≈ 30 atmospheres, a critical temperature $T_c \sim 10^{-2}$ °K and a ground state vacancy concentration of $\sim 10^{-4}$ are predicted near melting. Both quantities fall off rapidly with increasing pressure. The experimental consequences of such a vacancy concentration are discussed with the following results: The He^3-vacancy pairs are capable of accounting for the observed He^3 diffusion, and the pure solid may exhibit superfluidity below the critical temperature although this is not presently experimentally accessible for solid He^4.

The He^3-He^3 bound states are analyzed in a model involving only nearest neighbor exchange matrix elements J_{34} and J_{33}. The parameter J_{34} which had been previously reported to be $\sim 10^{-2}$-10^{-3} J_{33} (a ratio difficult to understand theoretically) is reanalyzed in light of the fact that for $J_{33} \gg J_{34}$, a He^3 molecule is formed. The diffusion data then give $J_{34} \sim 0.1\ J_{33}$. The triplet bound states are shown to give rise to two peaks in the NMR relaxation time data which are observed experimentally. A theoretical calculation of the relaxation time is shown to be in good agreement with experiment.

CHAPTER 1

INTRODUCTION

In solid He^4 crystals there is a large overlap of wave functions between He^4 nuclei on nearest neighbor lattice sites. This allows defects such as vacancies or He^3 impurities to move by exchange with a nearest neighbor He^4 atom. Classically such defects are regarded as localized objects which only occasionally move from one position to another. Andreev and Lifshitz (1) suggested that in solid helium defects might become delocalized through quantum mechanical exchange and move through the crystal in a coherent manner. These excitations are known as impuritons and vacancy waves.

Experiments on He^4 crystals with small amounts of He^3 impurities clearly showed the existence of impuritons. It is possible to follow the motion of He^3 impurities since they are tagged by their nuclear spin whereas the He^4 atoms have no spin. Thus, nuclear magnetic resonance (NMR) experiments are most useful in observing impuriton motion in solid helium. In the NMR experiments of Richards, Pope, and Widom (2) the diffusion of impurities was measured as a function of concentration. They found the relationship

$$D = D_o/X_3 \quad , \tag{1.1}$$

where D is the diffusion coefficient, D_o is a constant and X_3 is the concentration of He^3 impurities, i.e., $X_3\rho_o$ is the density of He^3 impurities; ρ_o is the number density of He^4. Their analysis of this result is as follows.

Classically the diffusion is governed by the random walk of an impurity on a lattice. Thus

$$D \sim \frac{J_{34}}{\hbar} \Delta^2 \quad , \tag{1.2}$$

where Δ is the nearest neighbor distance ($\rho_o = 1/\Delta^3$) and $J_{34}/\hbar$ is the He^3-He^4 exchange rate. In this case there is no dependence on X_3.

At sufficiently low temperatures phonon scattering is negligible (1) and the impuriton motion may be treated using the kinetic theory of a diffuse gas of particles. The impuriton-impuriton scattering is assumed to have a range R. The diffusion constant is then given by

$$D \sim v\lambda \quad , \tag{1.3}$$

where v is the group velocity ($\sim J_{34}\Delta/\hbar$) and λ is the mean free path. For λ we have

$$\lambda \sim \frac{\Delta^3}{X_3 R^2} \quad . \tag{1.4}$$

Therefore

$$D \sim \frac{J_{34}\Delta^4}{\hbar R^2 X_3} \quad , \tag{1.5}$$

with the correct X_3 dependence. Thus impuriton motion is accounts for the experimental observations.

Because of the smaller mass of the He^3 atom it has a larger zero point motion than a He^4 atom. Thus it will more readily exchange with a vacancy than would a He^4 atom. It will also tend to exchange with another He^3 atom more quickly than with a He^4 atom. This effect tends to produce binding between an impuriton and a vacancy wave in the first case and between impuritons in the second. However localizing an excitation tends to increase the system energy and work against the formation of a bound state. In either case there is then a critical exchange frequency necessary to produce binding. In Chapter 2 we treat these interactions in a cubic crystal with particular emphasis on the possible formation of impuriton-impuriton and impuriton-vacancy bound states. We find that both types of "molecule" probably exist (3).

The existence of impuriton-vacancy molecules has a very interesting experimental consequence. This molecule has a large mobility, comparable to that of the vacancy mobility, and much greater than the bare impuriton mobility. A small number of bound states can thus carry a large current of impurities and markedly affect the observed diffusion.

The NMR experiments of Miyoshi et al. (4) have quite clearly shown the existence of thermally activated vacancies in solid He^4. The concentration of thermally activated vacancies is

$$X_v \cong e^{-\beta\phi} \tag{1.6}$$

where ϕ is the activation energy, and $\beta = 1/k_B T$ (k_B is Boltzmann's constant). We find that as the temperature is increased the impuriton gas model becomes inapplicable. This model is only valid if an impuriton can undergo many coherent hops between lattice sites before it is scattered, i.e., $J_{34}\tau >> 1$, where τ is the scattering time.

A very small concentration of relatively high velocity vacancies will, however, cause $J_{34}\tau << 1$ and the resultant diffusion will be of the random walk type. Our analysis in Chapter 2 shows that vacancies alone should cause a sharp drop in the diffusion at temperatures and He^3 concentrations where no such drop has been observed. However when we add the diffusion current due to high mobility He^3-vacancy molecules we get a quite reasonable fit to the data.

In Chapter 3 we consider the possibility that ground state vacancies may exist in solid He^4, i.e., the activation energy ϕ may become negative. This phenomena appears to be linked to Bose-Einstein condensation in a solid. Penrose and Onsager (5) have concluded that the Bose condensate fraction is zero in a solid with one particle per site. However Chester (6, p. 258) has concluded ". . . a quantum crystal can have a Bose-Einstein condensate . . . if it has a finite concentration of vacancies." Furthermore, there is ". . . no reason, whatsoever, to suppose that a quantum crystal cannot have a finite fraction of vacancies at absolute zero (6, p. 258)."

There are, in fact, several reasons for believing that both solid He^3 and solid He^4 have $\sim 10^{-4}$ vacancies/site as $T \to 0$ °K on the melting curve:

a. Widom and Sokoloff (7) have shown that such a concentration of vacancies qualitatively resolves previous contradictions in estimating the solid He^4 Heisenberg exchange energy from thermal data.

b. Greywall (8) has examined the specific heat anomalies in solid He^3 and concludes that the solid may contain a "Landau-Fermi fluid" of $\sim 10^{-4}$ quasi-particles per site.

c. Leggett (9) has estimated the "superfluid fraction" in the Bose-condensed He^4 solid and finds $\sim 10^{-4}$ "superfluid particles" per site.

d. From an analysis of nuclear magnetic linewidths of He^3 impurities in solid He^4 Guyer (10) estimates $\sim 10^{-4}$ vacancies per site as an upper limit for x_o.

Widely different physical considerations thus lead to the same order of magnitude for the fraction of ground state vacancies in solid helium. This fact is in no way proof of the validity of the estimate. On the other hand, the above listed results are highly suggestive.

Chester also states that Bose-Einstein condensation in quantum crystals ". . . is unlikely to set in without a phase transition . . . , thus, we are led to speculate that there might be an undetected phase transition in the solid phase of He^4. It is, unfortunately, impossible to say where in the solid phase the transition might take place (6, p. 257)." This statement appears to us unduly pessimistic, and in Chapter 3 we attempt the task of computing the λ-transition for solid He^4.

Chapter 3 also contains arguments showing that a concentration $X_o \sim 10^{-4}$ of ground state vacancies is consistent with the experimental

diffusion. The impuriton gas model is inapplicable at this vacancy concentration. The diffusion is dominated by fast moving molecules which are mainly scattered by He^3 impurities. Our calculation gives diffusion of the right order of magnitude and proportional to X_3^{-1} in agreement with experiment. This strongly suggests that the experiment of Richards et al. (2) may have actually measured the diffusion of impuriton-vacancy molecules.

In Chapter 4 we analyze the experimental consequences of the existence of He^3-He^3 molecules in the impuriton gas model. In particular, we use our previous results to extract the He^3-He^4 exchange parameter (J_{34}) from the diffusion data. Richards et al. (2) reported a value $J_{34}/J_{33} \sim 10^{-2}$-$10^{-3}$ J_{33} where J_{33} is the He^3-He^3 exchange rate. One would expect $J_{34} < J_{33}$ as mentioned above; however, it does appear that J_{34} should be comparable to J_{33} since the mass difference does not seem to warrant factors of 10^{-2}-10^{-3}. Because an anomalously small J_{34} value seemed theoretically unacceptable a variety of long range crystal distortion models were proposed (11-14). The distortion around an impurity was expected to slow the movement of other impurities.

In Chapter 4 we develop the following results:

a. The NMR data can be explained using the model Hamiltonian of Chapter 2, whose only parameters are the nearest neighbor exchange matrix elements J_{34} and J_{33}, with no distortions.

b. The value of J_{34} is not as unreasonably small as reported previously.

c. The existence of impuriton-impuriton molecular states is indicated by the data. We believe that the latter molecules are of the type analyzed in Chapter 2. However a recent form of the distortion model (15) involving molecules of quite a different type also gives reasonable agreement with experiment.

Finally, in Chapter 5 we summarize our conclusions regarding the dynamics of He^3 atoms and vacancies in solid He^4, and discuss some possible extensions of the present calculations.

CHAPTER 2

EXISTENCE OF IMPURITON-IMPURITON AND IMPURITON-VACANCY BOUND STATES IN SOLID He^4

One-Dimensional Model Calculation

An example of a hopping-induced bound state is illustrated by the following one-dimensional calculation. Taking an extreme case where the He^3 is unable to hop unless a vacancy is adjacent to it, we have -t as the vacancy hopping amplitude in the bulk, while $-(t + \Delta t)$ is the amplitude to hop to the He^3 site. A delocalized vacancy state has a minimum and maximum energy $\simeq E_o \pm 2t$ (E_o = energy at center of band) while a localized state, adjacent to the He^3 can lower (and raise) its energy to $E_o \pm (t + \Delta t)$ by exchange with the He^3. Thus, for $\Delta t \gtrsim t$ we expect localized vacancy states with energies above and below the vacancy band.

Method of Treatment of the Problem

To extend the above calculation to a quantitative treatment of the 3-dimensional motion, we first treat the He^3-vacancy interaction, and then generalize the results to the He^3-He^3 interaction. In developing the Hamiltonian for this system we assume a simple cubic lattice. This is a good approximation for a body centered cubic (BCC) lattice but is only fair for a hexagonal close packed (HCP) lattice.

This point will be discussed at greater length in Chapter 4. We allow only nearest neighbor hopping and prohibit double occupancy of lattice sites. Finally we neglect the interaction induced by strain fields which may be set up by the vacancies and impurities. The results of Chapter 4 have thrown into doubt whether strain fields play any significant role in quantum crystals.

Model Hamiltonian

Our system is assumed to consist of one He^3 atom and one vacancy in an otherwise pure He^4 crystal. We introduce creation and annihilation operators for the two kinds of particles at each lattice site; b_i^+ and f_i^+ are creation operators for a He^4 atom and a He^3 atom respectively. The possible states of the system are taken to be $|\underset{\sim}{k},\underset{\sim}{\ell}\rangle = f_{\underset{\sim}{k}}^+ b_{\underset{\sim}{k}} b_{\underset{\sim}{\ell}}|0\rangle$, where $|0\rangle$ has all sites occupied by He^4 atoms. The scalar product is

$$\langle \underset{\sim}{\ell}', \underset{\sim}{k}' | \underset{\sim}{k}, \underset{\sim}{\ell} \rangle = \delta_{\underset{\sim}{k},\underset{\sim}{k}'} \, \delta_{\underset{\sim}{\ell},\underset{\sim}{\ell}'} \, (1 - \delta_{\underset{\sim}{k},\underset{\sim}{\ell}}) \quad .$$

The set of states is then orthonormal except for the null vector $|k,k\rangle$.

The model Hamiltonian for the He^3-vacancy system is

$$\mathcal{H} = - \sum_{ij} T_{ij} \, b_j^+ \, b_i - \sum_{ij} M_{ij} \, f_i^+ \, b_i \, b_j^+ \, f_j - \sum_{ij} B_{ij} \, f_i^+ \, f_j \quad . \qquad (2.1)$$

The terms describe vacancy hopping, He^3-He^4 exchange and He^3-vacancy exchange respectively. In our approximation

$$T_{ij}, \, M_{ij}, \, B_{ij} = \begin{cases} t, J_{34}, b & \text{(nearest neighbors)} \\ 0 & \text{(otherwise)} \end{cases} \quad .$$

In this chapter we measure t, J_{34}, and b in units of °K. In Chapter 4 we find that $J_{34} \cong 3 \times 10^{-6}$ °K. Mineev (16) has calculated the vacancy hopping amplitude for BCC He^3 and HCP He^4. For HCP He^4 at V = 2.10 cm^3/mole (Δ = 3.5 Å, Δ = nearest neighbor distance), he obtains t ≅ 0.1 °K. Guyer (17) finds that t ≅ 0.1 °K from experimental data. The parameter b may be estimated by assuming it equal to the vacancy hopping amplitude at the same Δ in BCC He^3. This yields b ≅ 0.5 °K; the experimental results (18) give b ≃ 0.2 - 0.6 °K.

$\mathcal{H}$ operating on the state $|\underset{\sim}{k}\ \underset{\sim}{\ell}\rangle$ can be written as $\mathcal{H}_o\ |\underset{\sim}{k}\ \underset{\sim}{\ell}\rangle + V\ |\underset{\sim}{k}\ \underset{\sim}{\ell}\rangle$ where:

$$\mathcal{H}_o|\underset{\sim}{k},\underset{\sim}{\ell}\rangle = -t \sum_{\underset{\sim}{\Delta}} |\underset{\sim}{k},\underset{\sim}{\ell}+\underset{\sim}{\Delta}\rangle - J_{34} \sum_{\underset{\sim}{\Delta}} |\underset{\sim}{k}+\underset{\sim}{\Delta},\underset{\sim}{\ell}\rangle \quad , \tag{2.2}$$

$$\begin{aligned} V|\underset{\sim}{k},\underset{\sim}{\ell}\rangle = {} & t \sum_{\underset{\sim}{\Delta}} (\delta_{\underset{\sim}{k},\underset{\sim}{\ell}} + \delta_{\underset{\sim}{k},\underset{\sim}{\ell}+\underset{\sim}{\Delta}}) |\underset{\sim}{k},\underset{\sim}{\ell}+\underset{\sim}{\Delta}\rangle \\ & - b \sum_{\underset{\sim}{\Delta}} \delta_{\underset{\sim}{\ell},\underset{\sim}{k}+\underset{\sim}{\Delta}} |\underset{\sim}{k},\underset{\sim}{\ell}\rangle + J_{34} \sum_{\underset{\sim}{\Delta}} (\delta_{\underset{\sim}{k},\underset{\sim}{\ell}} + \delta_{\underset{\sim}{k}+\underset{\sim}{\Delta},\underset{\sim}{\ell}}) |\underset{\sim}{k}+\underset{\sim}{\Delta},\underset{\sim}{\ell}\rangle \quad , \end{aligned} \tag{2.3}$$

and the $\sum_{\underset{\sim}{\Delta}}$ indicates a summation over all nearest neighbors. We have used the fact that $|\underset{\sim}{k},\underset{\sim}{k}\rangle$ is the null vector to write $\mathcal{H}|\underset{\sim}{k},\underset{\sim}{\ell}\rangle$ in this way. We can now adjoin this vector to the vector space without affecting the physical results since there are no matrix elements between the unphysical state and the physical ones. $\mathcal{H}_o$ can then be diagonalized in terms of a vacancy wave and a mass fluctuation wave as shown below.

Solution of the Model Hamiltonian

Diagonalization of $\mathcal{H}_o$

Since the impurity-vacancy interaction depends only on the relative coordinates we switch to the conjugate coordinates in position space: $\underset{\sim}{C} = \frac{1}{2}(\underset{\sim}{k}+\underset{\sim}{\ell})$ and $R = \underset{\sim}{k}-\underset{\sim}{\ell}$. Then equations 2.2 and 2.3 become

$$\mathcal{H}_o|\underset{\sim}{C},\underset{\sim}{R}\rangle = -t \sum_{\underset{\sim}{\Delta}} |\underset{\sim}{C}+\tfrac{1}{2}\underset{\sim}{\Delta},\underset{\sim}{R}-\underset{\sim}{\Delta}\rangle - J_{34} \sum_{\underset{\sim}{\Delta}} |\underset{\sim}{C}+\tfrac{1}{2}\underset{\sim}{\Delta},\underset{\sim}{R}+\underset{\sim}{\Delta}\rangle \quad , \tag{2.4}$$

and

$$\begin{aligned} V|\underset{\sim}{C},\underset{\sim}{R}\rangle = {} & t \sum_{\underset{\sim}{\Delta}} (\delta_{\underset{\sim}{R},0} + \delta_{\underset{\sim}{R},\underset{\sim}{\Delta}}) |\underset{\sim}{C}+\tfrac{1}{2}\underset{\sim}{\Delta},\underset{\sim}{R}-\underset{\sim}{\Delta}\rangle \\ & + J_{34} \sum_{\underset{\sim}{\Delta}} (\delta_{\underset{\sim}{R},\underset{\sim}{0}} + \delta_{\underset{\sim}{R},-\underset{\sim}{\Delta}}) |\underset{\sim}{C}+\tfrac{1}{2}\underset{\sim}{\Delta},\underset{\sim}{R}+\underset{\sim}{\Delta}\rangle - b \sum_{\underset{\sim}{\Delta}} \delta_{\underset{\sim}{R},-\underset{\sim}{\Delta}} |\underset{\sim}{C},-\underset{\sim}{R}\rangle \quad . \end{aligned} \tag{2.5}$$

In terms of a mixed basis set defined by

$$|\underset{\sim}{K},\underset{\sim}{R}\rangle = (2N)^{-\frac{1}{2}} \sum_{\underset{\sim}{\Delta}} \exp(i\underset{\sim}{K}\cdot\underset{\sim}{C}) |\underset{\sim}{C},\underset{\sim}{R}\rangle \quad , \tag{2.6}$$

(N = number of unit cells), equations 2.4 and 2.5 may be written as

$$\begin{aligned} \mathcal{H}_o|\underset{\sim}{K},\underset{\sim}{R}\rangle = {} & -t \sum_{\underset{\sim}{\Delta}} \exp(-i\tfrac{1}{2}\underset{\sim}{K}\cdot\underset{\sim}{\Delta}) |\underset{\sim}{K},\underset{\sim}{R}-\underset{\sim}{\Delta}\rangle \\ & - J_{34} \sum_{\underset{\sim}{\Delta}} \exp(-i\tfrac{1}{2}\underset{\sim}{K}\cdot\underset{\sim}{\Delta}) |\underset{\sim}{K},\underset{\sim}{R}+\underset{\sim}{\Delta}\rangle \quad , \end{aligned} \tag{2.7}$$

and

$$V|\underset{\sim}{K},\underset{\sim}{R}\rangle = t \sum_{\underset{\sim}{\Delta}}(\delta_{\underset{\sim}{R},0} + \delta_{\underset{\sim}{R},\underset{\sim}{\Delta}}) \exp(-i\tfrac{1}{2}\underset{\sim}{K}\cdot\underset{\sim}{\Delta})|\underset{\sim}{K},\underset{\sim}{R}-\underset{\sim}{\Delta}\rangle + J_{34} \sum_{\underset{\sim}{\Delta}}(\delta_{\underset{\sim}{R},0} + \delta_{\underset{\sim}{R},-\underset{\sim}{\Delta}}) \exp(-i\tfrac{1}{2}\underset{\sim}{K}\cdot\underset{\sim}{\Delta})|\underset{\sim}{K},\underset{\sim}{R}+\underset{\sim}{\Delta}\rangle - b \sum_{\underset{\sim}{\Delta}} \delta_{\underset{\sim}{R},\underset{\sim}{\Delta}}|\underset{\sim}{K},-\underset{\sim}{R}\rangle \quad . \tag{2.8}$$

We now define a state vector $|\underset{\sim}{K}\ \underset{\sim}{\tau}\rangle$ where $\underset{\sim}{\tau}$ is a relative wave vector:

$$|\underset{\sim}{K},\underset{\sim}{\tau}\rangle = N^{-\frac{1}{2}} \sum_{\underset{\sim}{R}} \exp(i\underset{\sim}{\tau}\cdot\underset{\sim}{R})|(\underset{\sim}{K},\underset{\sim}{R}\rangle \quad . \tag{2.9}$$

Operating on this state vector with $\mathcal{H}_o$ gives:

$$\mathcal{H}_o|\underset{\sim}{K},\underset{\sim}{\tau}\rangle = -t \sum_{\underset{\sim}{\Delta}} \{\exp[i(\underset{\sim}{\tau}-\tfrac{1}{2}\underset{\sim}{K})\cdot\underset{\sim}{\Delta}]\}|\underset{\sim}{K},\underset{\sim}{\tau}\rangle - J_{34} \sum_{\underset{\sim}{\Delta}} \{\exp[-i(\underset{\sim}{\tau}+\tfrac{1}{2}\underset{\sim}{K})\cdot\underset{\sim}{\Delta}]\}|\underset{\sim}{K},\underset{\sim}{\tau}\rangle \quad . \tag{2.10}$$

$\mathcal{H}_o$ is thus diagonalized in terms of a vacancy wave of wave vector $\underset{\sim}{\lambda} = \underset{\sim}{\tau} + \underset{\sim}{K}/2$ and a mass fluctuation wave with $\underset{\sim}{\lambda}' = -\underset{\sim}{\tau} + \underset{\sim}{K}/2$, where $\underset{\sim}{\tau}$ is the relative wave vector $(\underset{\sim}{\lambda}-\underset{\sim}{\lambda}')/2$ and $\underset{\sim}{K}$ is the total wave vector $\underset{\sim}{\lambda}+\underset{\sim}{\lambda}'$.

Calculation of Bound States and Scattering Lifetimes

To compute the bound states and scattering lifetimes we follow the method developed by Boyd and Callaway (19) to deal with short range

interactions between excitations in a solid. We begin by writing the Lippmann-Schwinger (20) equation as

$$\psi = u + GV\psi \quad , \tag{2.11}$$

where u is an eigenfunction of $\mathcal{H}_o$ with energy E and the Green's function is $G = (E - \mathcal{H}_o + i\varepsilon)^{-1}$. A formal solution to equation 2.11 is given by

$$\psi = u + GV(1-GV)^{-1} u \quad . \tag{2.12}$$

If u = 0 in equation 2.12 we may still have a finite ψ if

$$\det (1-GV) = 0 \quad . \tag{2.13}$$

Such a solution would correspond to a bound state at the energy for which equation 2.13 is satisfied. The remainder of the calculation involves the tedious process of evaluating the above determinant. The details of the calculation are given in Appendix A. In what follows we shall merely quote the results of the calculation.

We define $A_{jk\ell}$ by

$$A_{jk\ell} = \lim_{\varepsilon \to 0^+} \frac{-i}{a} \, i^{(j+k+\ell)} \int_o^\infty d\beta \; e^{i(E+i\varepsilon)} \; J_j(\beta) \; J_k(\beta) \; J_\ell(\beta) \quad , \tag{2.14}$$

where $a = 2t$ and $J_n(\beta)$ is a Bessel function. Using this definition we may write the determinant of equation 2.13 for $\underset{\sim}{K} = 0$ as $D_o\, D_1^2\, D_2^3$ where

$$D_o = a(1 - 3aA_{001})\,[1 - 3aA_{001} + b(A_{000} + 4A_{001} + A_{002})]$$
$$- 1.5\,(aA_{000} - 2bA_{001})\,(A_{000} + 4A_{001} + A_{002}) \quad ,$$
$$D_1 = 1 + b(A_{002} - A_{000}) \quad , \qquad (2.15)$$
$$D_2 = 1 + b(A_{000} + A_{002} - 2A_{011}) \quad .$$

D_o refers to s-like states, D_1 to p-like states and D_2 to d-like states (21). The solutions to equation 2.13 are shown as a function of b/t in figures 1 and 2 for above-and below-band bound states respectively. The A's were evaluated numerically by computer with an upper limit of 70 and an interval of 0.005. These values agreed with those found in the literature (21). The calculation is accurate to a few percent.

Inside the continuum $D_\beta \neq 0$ ($\beta = 0,1,2$). However a scattering resonance occurs if $\mathrm{Re}(D_\beta) = 0$ and the width Γ is positive. The energy and width is given by (18)

$$E_{\beta,r} = E_{\beta,0} - \frac{D_{\beta,i}\, D'_{\beta,i}}{(D'_{\beta,r})^2 + (D'_{\beta,i})^2} \quad , \qquad \Gamma_\beta = \frac{2\, D_{\beta,i}\, D'_{\beta,r}}{(D'_{\beta,r})^2 + (D'_{\beta,i})^2} \quad ,$$

(2.16)

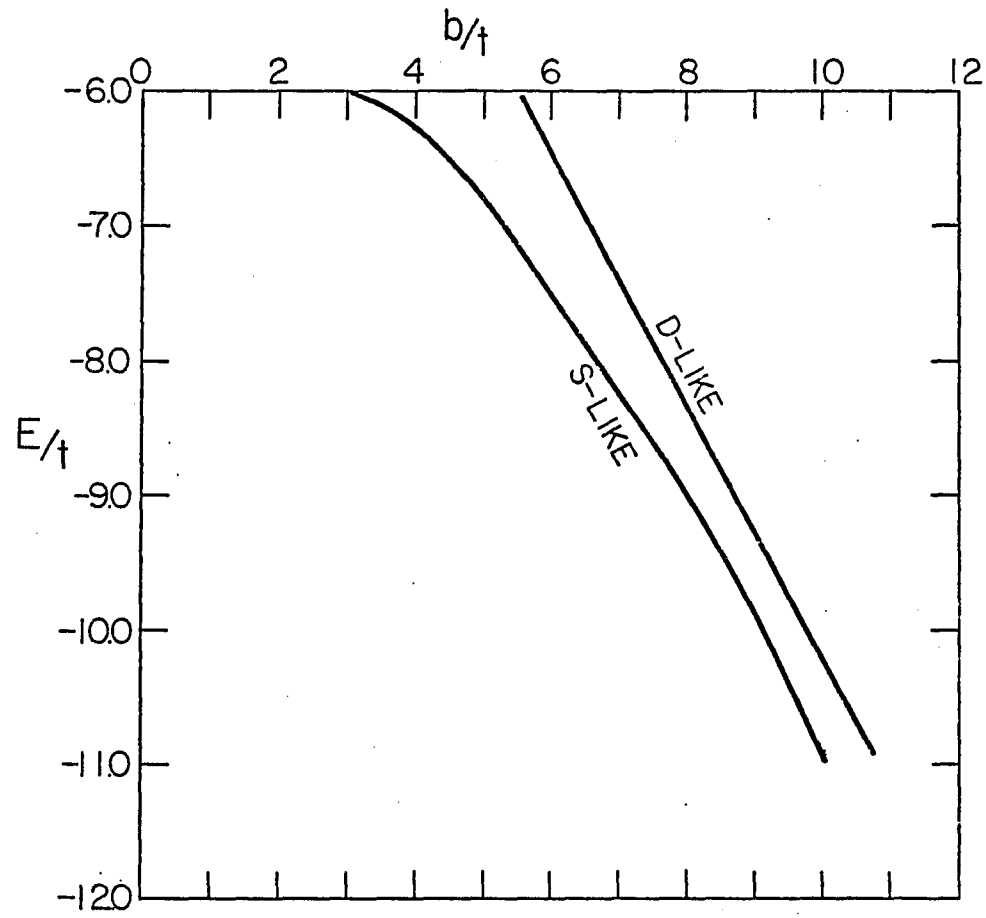

Fig. 1. Energy of below-band vacancy-He^3 bound states in solid He^4. The ratio b/t is the ratio of He^3-vacancy exchange to He^4-vacancy exchange, and is expected to be ≈ 5 for HCP He^4 at a density of 2.10 cm^3/mole. The bottom of the unperturbed vacancy band is at E/t = -6.

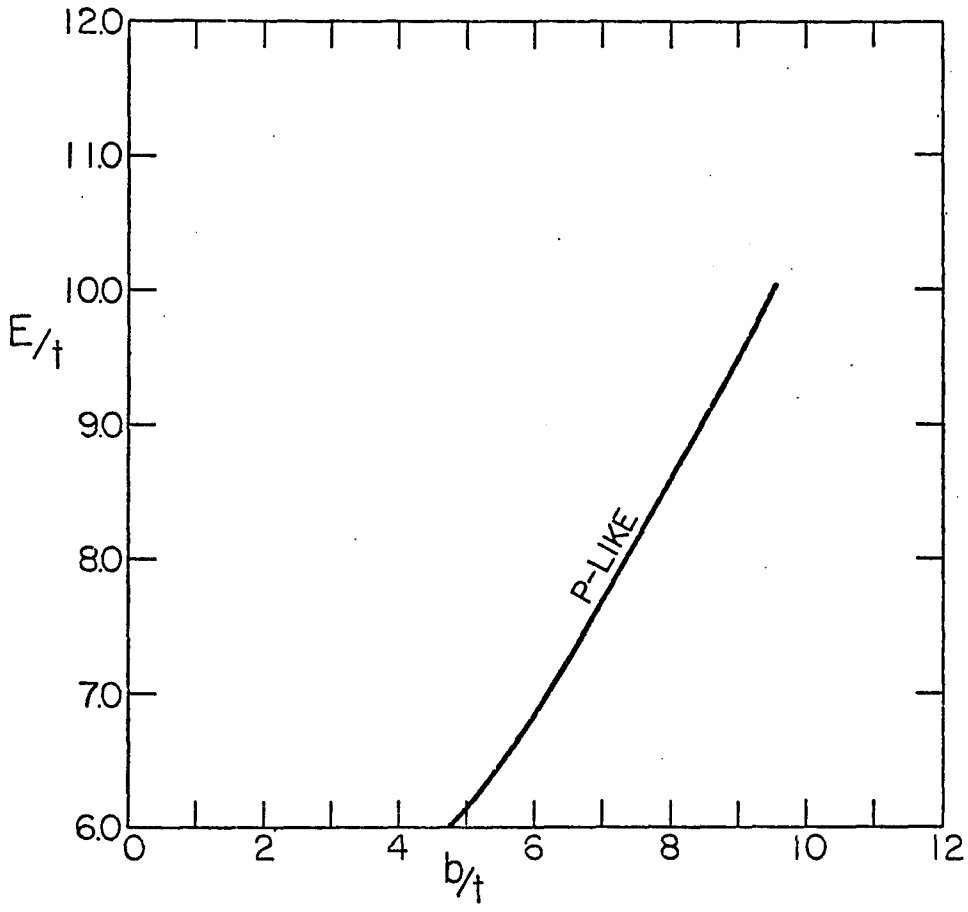

Fig. 2. Energy of above-band vacancy-He^3 bound states in solid He^4.

The top of the unperturbed vacancy band is at E/t = 6. These states are p-like.

where $D_{\beta r}$ and $D_{\beta i}$ are the real and imaginary parts of D_o, D_1 or D_2. The prime indicates differentiation with respect to energy, and $E_{\beta o}$ is the energy for which $Re(D_\beta) = 0$. The results for resonance energies and widths as a function of b/t are shown in figure 3.

For $\underset{\sim}{K} \neq 0$ the determinant of equation 2.13 is given by B^2C where

$$\begin{aligned} B &= A_{55}\,(A_{11}A_{22} - A_{12}A_{21}) + A_{52}\,(A_{15}A_{21} - A_{11}A_{25}) \quad , \\ C &= A_{33}A_{55} - A_{36}A_{52} \quad , \end{aligned} \tag{2.17}$$

and A_{ij} is the ij^{th} matrix element of the matrix given in equation A.15 of Appendix A. The results for the energies of bound states and scattering resonances below and above the band, as a function of $\underset{\sim}{K}$, for various values of b/t are shown in figures 4 and 5 respectively.

It should be noted here that the bandwidth for a bound state is $\cong$ t so that an impurity has much greater mobility in this bound state ($t >> J_{34}$). A rough physical picture of this effect is to imagine a He^3-V exchange, the vacancy then moving around the He^3 back to the other side and repeating the process. This process yields an effective hopping amplitude for the bound state $t' \approx t/2z$ where z = 6 for a cubic crystal. This effective hopping amplitude can be used to estimate the band width in BCC and HCP He^4 by multiplying by 16 and 24 respectively. The effect of the bound state and resonant scattering would be to <u>increase</u> the diffusion of He^3 with temperature by providing more vacancies to enhance the He^3 hopping rate.

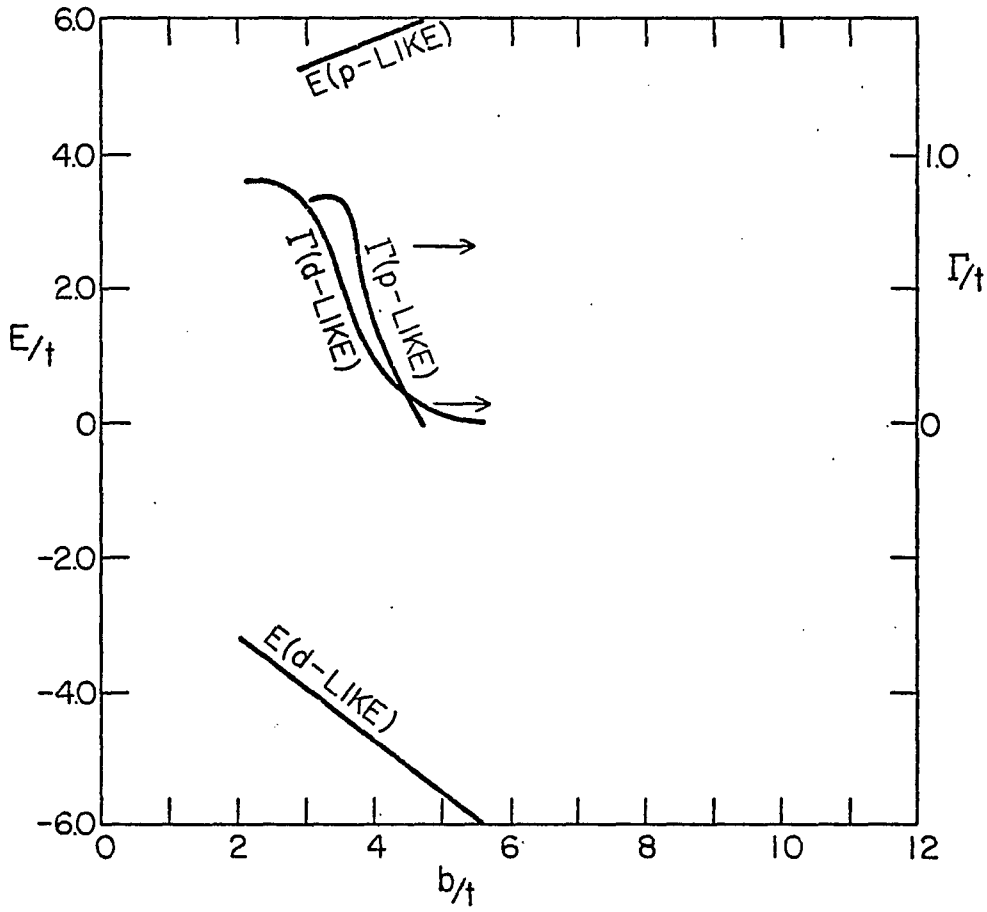

Fig. 3. Resonance widths and energies for K = 0 vacancy-He^3 scattering.

K is the center of mass crystal momentum. The vacancy band width in the absence of He^3 is 12 t.

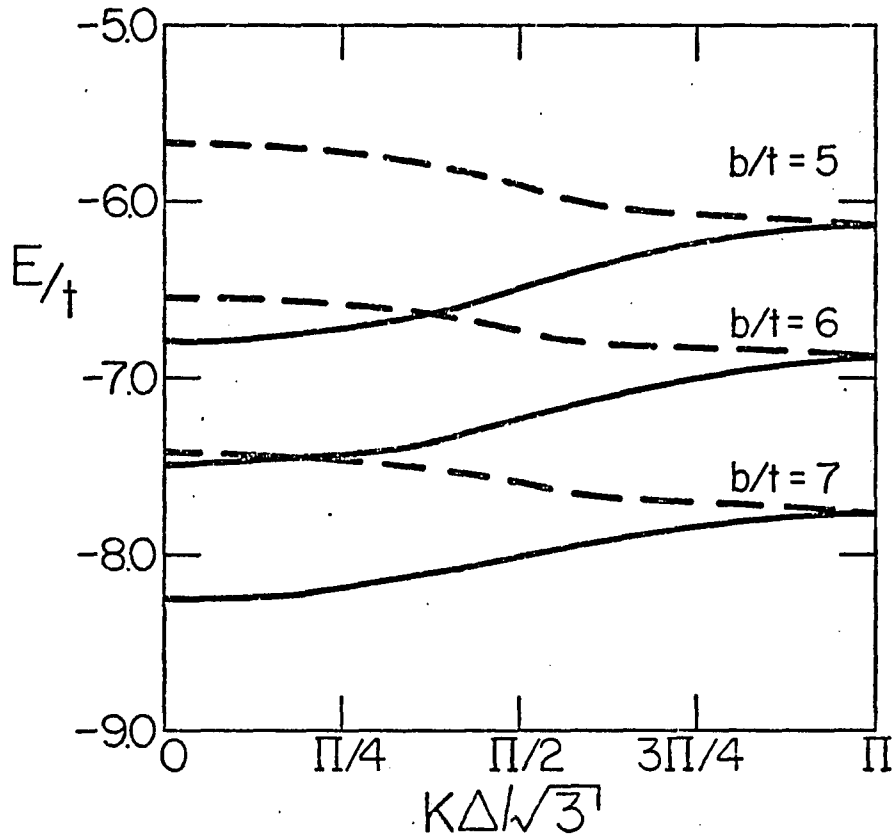

Fig. 4. Below-band vacancy-He^3 bound states (and resonances) as a function of $\underline{K}$.

K is the center of mass crystal momentum and is taken along the [1,1,1] direction. Δ is the lattice constant. The solid lines are s-like; the dashed lines are d-like states.

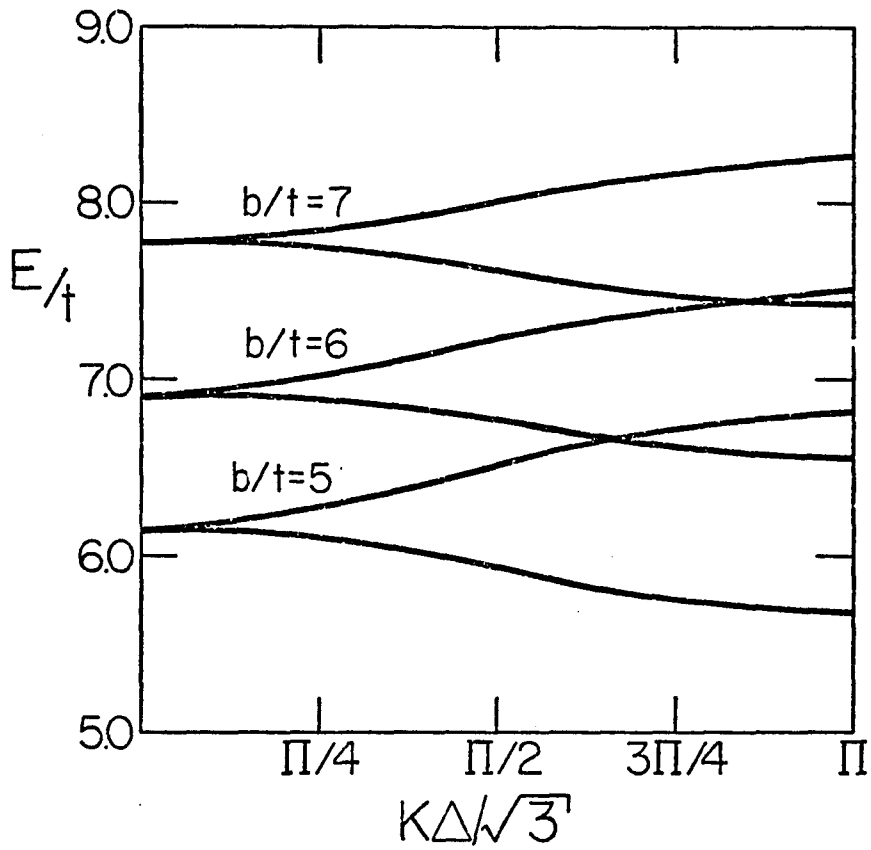

Fig. 5. Above-band vacancy-He^3 bound states (and resonances) as a function of $\underline{K}$ ($\underline{K}||[1,1,1]$).

The notation is the same as in Fig. 4.

Impuriton-Impuriton Bound States in Solid He^4

If $J_{33}/J_{34} > n$ where n is some critical value, a He^3-He^3 bound state will be produced in the same way as before. The Hamiltonian for this system is

$$\mathcal{H} = - \sum_{\sigma\langle ij\rangle} J_{34}\, f_{i\sigma}^{+}\, b_i\, b_j^{+}\, f_{j\sigma} - \sum_{\langle ij\rangle\sigma\sigma'} J_{33}\, f_{i\sigma}^{+}\, f_{j\sigma'}^{+}\, f_{i\sigma'}\, f_{j\sigma} \quad . \tag{2.18}$$

We neglect the dipole-dipole interaction, σ,σ' are the spin indices and $\langle ij\rangle$ means to sum over nearest neighbors only. The basis states in this case are $|\underset{\sim}{k}\sigma,\underset{\sim}{\ell}\sigma'\rangle = f_{\underset{\sim}{k}\sigma}^{+}\, b_{\underset{\sim}{k}}\, f_{\underset{\sim}{\ell}\sigma'}\, b_{\underset{\sim}{\ell}}|0\rangle$.

We solve this problem in almost exactly the same way as the vacancy-impuriton problem. First we consider the particles as distinguishable and drop the spin indices. We can then identify the molecules at the end as triplet or singlet by considering whether the space part of the wave function is symmetric or antisymmetric.

The details are in Appendix A. The result for K = 0 in the vacancy-impuriton problem is shown to be applicable to the He^3-He^4 system for all K in the (1,1,1) direction where $a = 4J_{34} \cos \frac{1}{2} \frac{K\Delta}{\sqrt{3}}$ and $b = J_{33}$ in equation 2.15 above.

The bound states are plotted in figure 6. The p-like states are the triplet spin states and the s- and d-like are the singlet.

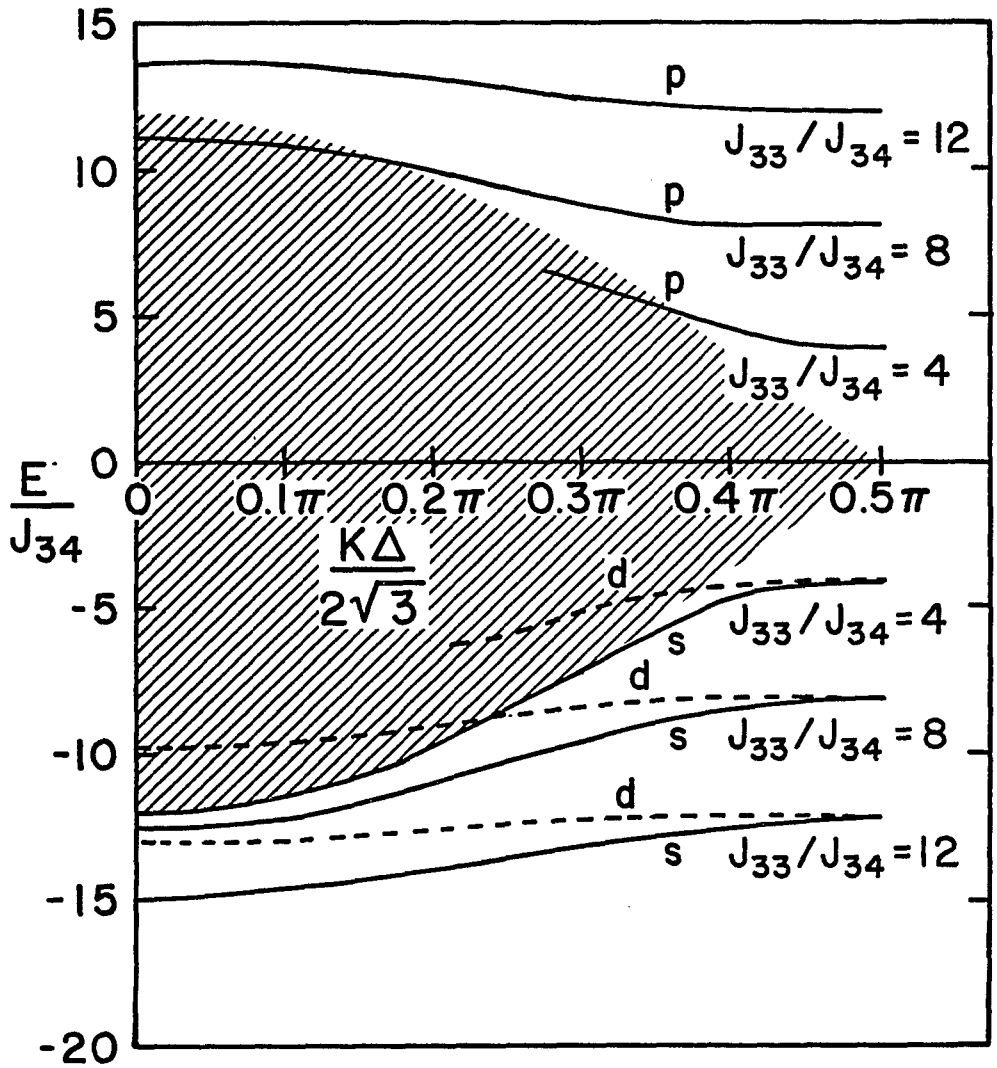

Fig. 6. The impuriton-impuriton resonances and bound states for J_{33}/J_{34} = 4, 8 and 12, plotted as a function of K.

Experimental Consequences of He^3-Vacancy Bound States

It appears likely that one or more vacancy-He^3 bound states exist in solid He^4 with binding energies ranging up to ≈ 0.2 °K. An estimate of the effects of these bound states on the diffusion of He^3 may be obtained by the following simplified analysis. Let N be the number of He^4 atoms in the crystal and $X_V N$ and $X_3 N$ the number of vacancies and He^3 impurities present. A single vacancy and impurity have N^2 possible states of which $\approx 6N$ (1 "s" state, 3 "p" states, and 2 "d" states) are bound. Thus the number of vacancy states that are bound for one He^3 is ~ 6. If we have $X_3 N$ impurities then each vacancy has ~ 6 $X_3 N$ possible bound states ($X_V << X_3$) and the fraction of vacancy states that are bound is $\sim 6\ X_3$. If there are $X_V N$ vacancies present then there will be $\sim 6\ X_3\ X_V N$ bound states (at temperatures such that $T \gtrsim t, E_{binding}$) and thus a fraction $\sim 6\ X_V$ of the He^3 states are bound.

The diffusion constant of He^3 in the presence of vacancies and He^3-vacancy molecules can be estimated as follows. The total diffusion constant is

$$D = D_I + n_b\ X_V\ D_M \quad , \tag{2.19}$$

where D_I is the diffusion constant of impuritons. D_M is the diffusion constant of molecules and n_b is the number of bound states. From simple diffusion theory

$$\frac{1}{D_I} = \frac{1}{D_{IV}} + \frac{1}{D_{II}} \quad , \tag{2.20}$$

where D_{II} is the diffusion constant in the presence of impuritons alone and D_{IV} is the diffusion constant of one impuriton in the presence of vacancies. Similarly

$$\frac{1}{D_M} = \frac{1}{D_{MV}} + \frac{1}{D_{MI}} \quad , \tag{2.21}$$

where D_{MV} and D_{MI} are the diffusion constants of He^3-vacancy molecules analogous to those above. D_{II} is calculated in Appendix B and is found to be given by

$$D_{II} = \frac{\pi}{8\hbar} \frac{J_{34}\,\Delta^2}{X_3\,\sigma^*} \quad . \tag{2.22}$$

The three other quantities are calculated in the same way. The results are:

$$D_{IV} = \frac{\pi}{4\hbar} \frac{J_{34}^2\,\Delta^2}{X_v t\,\sigma^*} \quad , \tag{2.23a}$$

$$D_{MV} = \frac{\pi}{4\hbar} \frac{(t')^2\,\Delta^2}{X_v(t+t')\,\sigma^*} \quad , \tag{2.23b}$$

$$D_{MI} = \frac{\pi}{4\hbar} \frac{t'\,\Delta^2}{X_3\,\sigma^*} \quad . \tag{2.23c}$$

In the above expressions t' is the hopping amplitude for He^3-vacancy molecules and $\sigma^* \Delta^2$ is the scattering cross section between the excitations considered. We are making the approximation that σ^* is the same ($\sigma^* \simeq 10$) regardless of which excitations are interacting. In addition, we are assuming the lifetime of a He^3-vacancy molecule to be

much larger than its collision time so that we may consider the molecule as a well-defined excitation of the He^3-He^4 crystal.

The general form of the results quoted in equations 2.22 and 2.23 may be understood by the following simplified argument. Suppose we wish to calculate D_{IV}, i.e., the diffusion of impurities as determined by scattering from vacancies. We can imagine sitting on an impuriton; since the vacancy has a much high velocity than an impuriton we would see a flux of vacancies given by $(\rho_o X_v)(t\Delta/\hbar)$ where $\rho_o X_v$ is the density of vacancies and $t\Delta/\hbar \approx$ the velocity of the vacancies. If we multiply this flux by the scattering cross section $\sigma^* \Delta^2$ we get the reciprocal of the scattering lifetime of the impuriton, i.e.,

$$1/\tau = (\rho_o X_v)(t\Delta/\hbar)\ \sigma^*\ \Delta^2 \quad .$$

Since the velocity of an impuriton is $\approx J_{34}\Delta/\hbar$ the mean free path for the impuriton (Λ) is given by $J_{34}\Delta\tau/\hbar$, and the diffusion constant is

$$J_{34}\Delta\Lambda/\hbar = \frac{1}{X_v \hbar}\ \frac{J_{34}^{\ 2}\ \Delta^2}{t\sigma^*}$$

which, neglecting factors of order $\pi/4$, is in agreement with equation 2.23a.

The result for the total diffusion constant is, from equations 2.19-2.23,

$$D = \left\{ \frac{2X_3\ J_{34}}{X_v t + 2X_3\ J_{34}} + \frac{2n_b\ X_3\ X_v (t')^2}{(X_3 t' + X_v(t+t')^2\ J_{34}} \right\} D_{II} \quad . \qquad (2.24)$$

To compare this expression with the experimental data we choose values of the various parameters that are in accord with theory and experiment. The vacancy activation energy is (4) ϕ = 15-18 °K. We use a somewhat higher value of t' than given above. Sacco and Widom (22) have shown that the molecular bandwidth of a very tightly bound impuriton-impuriton molecule in a HCP lattice is one fourth the scattering bandwidth. We therefore prefer the value t' = 0.25 t. The values used are t = 0.004 °K, n_b = 12, t' = 0.01 °K, ϕ = 17 °K and $J_{34} = 4 \times 10^{-6}$ °K. The result is plotted in figure 7 along with the experimental data of Grigoriev et al. (23).

Qualitatively the curves are explained as follows. As the vacancy concentration increases it becomes more likely for an impuriton to be scattered by a vacancy thus shortening the mean free path and decreasing the diffusion. However molecular diffusion increases due to the high velocity of molecules. These molecules are mainly scattered by impurities. The diffusion increases exponentially, completely dominated by the molecules. At higher temperatures the vacancy concentration will become large enough to dominate the scattering of the He^3-vacancy molecules. In this regime the diffusion constant will saturate to a constant value given by $n_b X_v D_{MV}$. At still higher temperatures the effects of phonon scattering would cause the diffusion constant to fall with temperature. For simplicity we do not include the effects of phonons. A complete theory would have to include their effect at the highest temperatures. Grigoriev et al. (23) attribute the slight drop at high temperature to phonons but do not consider the effects of vacancies.

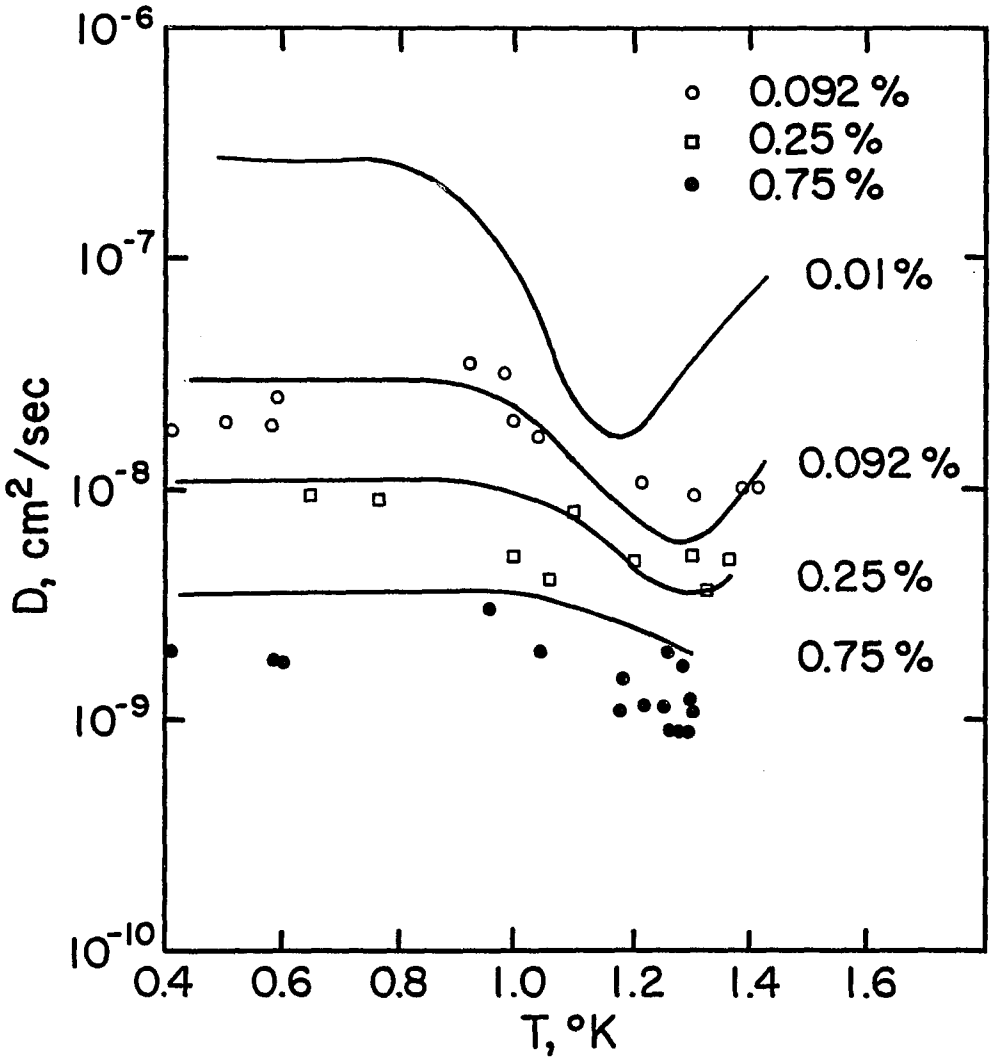

Fig. 7. The diffusion constant of impuritons plotted as a function of temperature for He^3 concentrations of 0.75%, 0.25%, 0.092% and 0.01%.

The solid lines are the theoretical dependence obtained from equation 2.24. The experimental points are taken from Grigoriev et al. (23).

If no bound state exists it appears that the diffusion should drop quite drastically at high temperatures. The fact that no such drop is seen is strong, though inconclusive, evidence for the existence of the bound state. However if slightly higher resolution of the data or experiments at slightly lower concentrations show the existence of a minima, after a drop of about an order of magnitude, the existence of an impurity-vacancy molecule will be clearly established.

Recent data suggest the bound state may not be stable in the HCP phase but does exist in the body centered cubic (BCC) phase of solid He^4. In figure 8 we show the diffusion data of Grigoriev, Esel'son and Mikheev (24) along the melting curve for a He^3 concentration of 0.75%. Since the BCC phase at this concentration occupies only a small sliver of the P-T plane the data go from HCP at low temperature to BCC and back to HCP at high temperature. A surprising jump of the diffusion coefficient occurs upon passing into the BCC phase from either the low or high temperature side. Also in the BCC phase there is a noticeable temperature dependence unlike the data for pure He^3 (25) and concentrated solutions (4).

According to Grigoriev et al. (24) this behavior cannot be explained by a difference in ϕ between the two phases since they find $\phi \cong 10\ ^\circ K$ in either phase. The large jump and the temperature dependence are easily understood if we assume that the diffusion is dominated by impuriton-vacancy molecules in the BCC phase but that impuritons do not bind to vacancies in the HCP phase. First we consider the BCC phase. In figure 9 we plot a theoretical curve

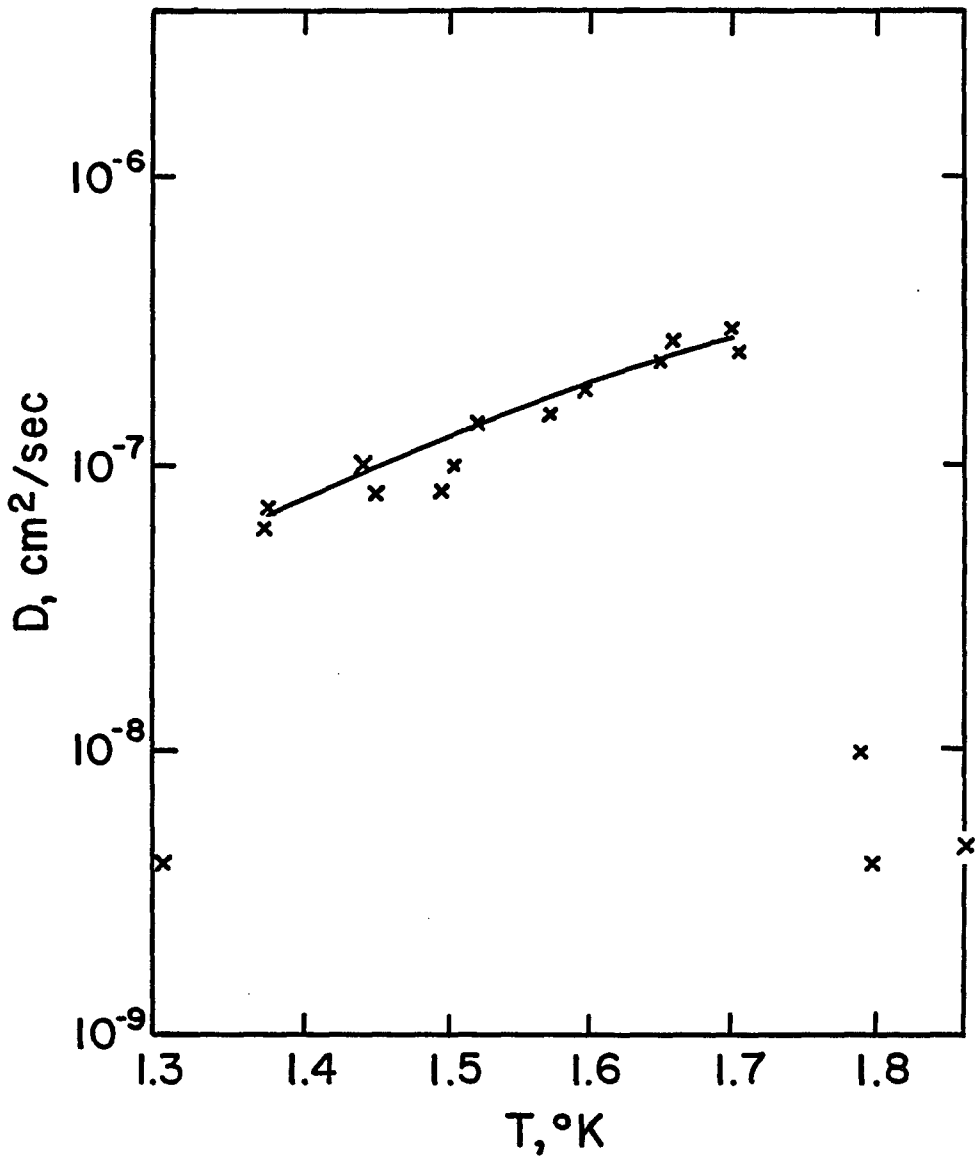

Fig. 8. Diffusion constant of He^3 along the melting curve of solid He^4.

The solid line is the theoretical result obtained from equations 2.25 and 2.27. The points are the experimental results. The He^3 concentration is 0.75%.

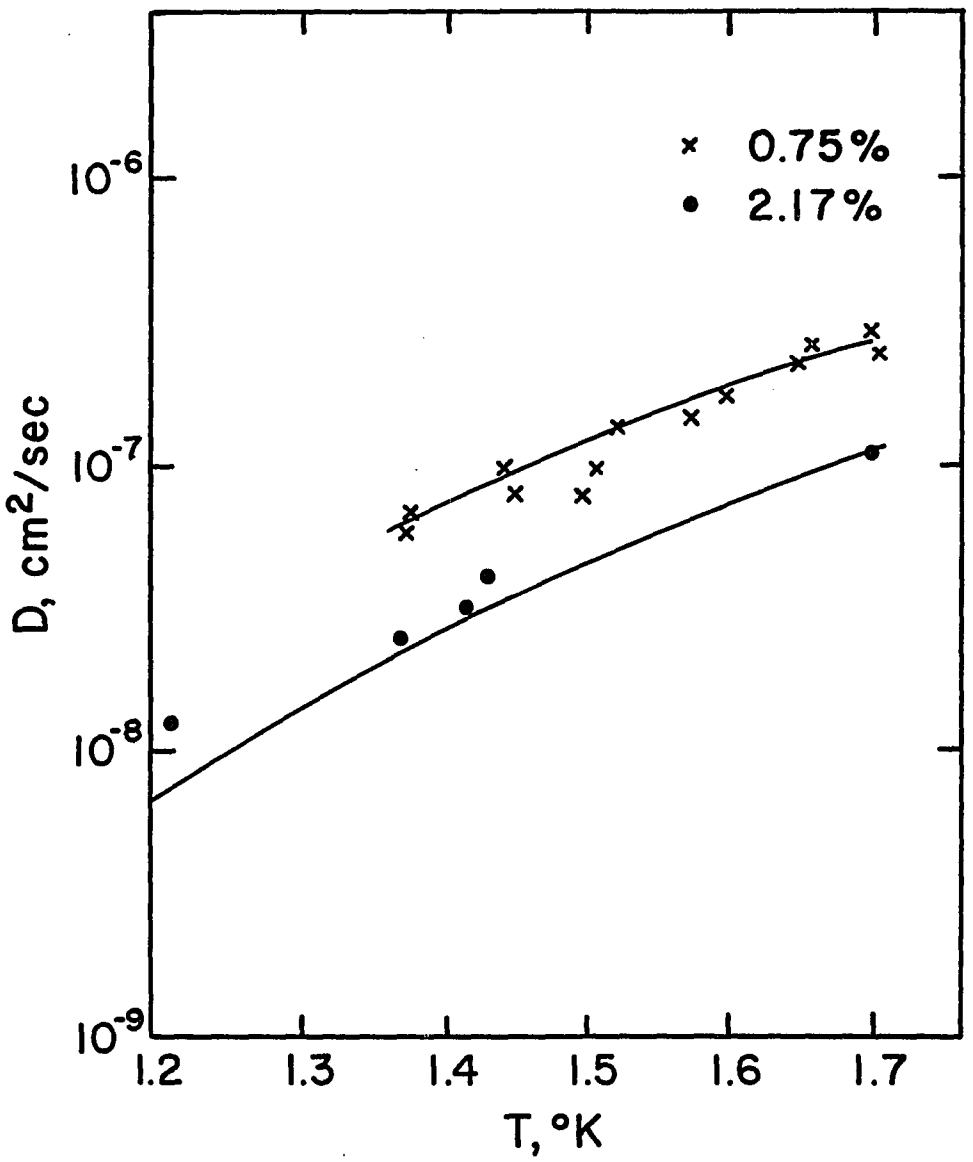

Fig. 9. Temperature dependence of the He^3 diffusion constant for two different He^3 concentrations.

The solid lines are theoretical curves obtained from equation 2.25.

using reasonable values of the various parameters: $t = 0.1\ ^\circ K$, $n_b = 8$ (there are eight nearest neighbors in the BCC lattice), $t' = 0.02\ ^\circ K$, $\phi = 11.5\ ^\circ K$, $\Delta = 3.6$ Å, and $J_{34} = 4 \times 10^{-6}\ ^\circ K$. Also since the molecule is unlikely to bind to a vacancy but likely to bind to an impuriton we take the cross section to be smaller in the first case. The actual numbers used were $\sigma^*_{MV} = 2.5$ for the first case and $\sigma^*_{MI} = 10$ for the second case. With these values the first term in equation 2.24, within the temperature range of existence of the BCC phase, is negligible compared to the second. With the adjustment of the cross sections the second term becomes

$$D = \frac{2n_b\, X_3\, X_v(t')^2\, D_{II}}{X_3 t' + 0.25\, X_v(t+t')J_{34}} \quad . \tag{2.25}$$

For the HCP phase, assuming no bound impuritons, the diffusion is given by the first term in equation 2.24 plus an additional term to describe the diffusion caused by random hops induced by vacancy-impurity exchange. We replace J_{34} by $X_v t$ in equation 2.1 to find

$$D_R \sim X_v t\, \Delta^2 \quad . \tag{2.26}$$

To fit the data both here and in figure 7 without bound states we need to take a small value of the impurity-vacancy cross section. Using $\sigma^*_{IV} = 0.01$ the diffusion constant in the HCP phase is fit reasonably well by

$$D \sim \frac{2X_3 J_{34}}{0.01X_v t + 2X_3 J_{34}} + X_v t \Delta^2 \quad . \qquad (2.27)$$

Another test of the theory would be to vary X_3 and see if the diffusion in the BCC phase varies according to equation 2.25. Without a bound state the diffusion would be given by equation 2.26 which is independent of X_3. In figure 9 we plot the data of Grigoriev et al. (24) for He^3 concentrations of 0.75% and 2.17% along with the curves given by equation 2.25. The agreement seems to be a futher confirmation of the theory.

The data are, however, too sketchy and too often conflicting to make any clear determination at this time. For example we quoted Miyoshi et al. (4) as giving ϕ_{HCP} = 15-18 °K in the HCP phase at V = 2.10 cm^3/mole whereas Grigoriev et al. (24) find ϕ_{HCP} = 10 °K at the same volume. However both sources agree that ϕ_{BCC} = 10 °K at the same volume. If the former result for ϕ_{HCP} proves correct the change in ϕ on crossing the BCC-HCP boundary could be the explanation for the diffusion jump at the transition. Furthermore the results of Grigoriev et al. (24) for V = 20.7 cm^3/mole in the HCP phase show thermal activation ($D \propto e^{-\beta\phi}$) and approximately an inverse proportionality of the diffusion coefficient to X_3 just as given by equation 2.25 as shown for the BCC phase in figure 9. Thus the idea that bound states exist in the HCP phase cannot be ruled out. Further experimentation is necessary. In particular, agreement on the value of ϕ_{HCP} must be reached and

diffusion data on somewhat smaller concentrations than are now experimentally accessible will be needed to resolve these questions.

CHAPTER 3

BOSE-EINSTEIN VACANCY CONDENSATION IN SOLID He^4

Vacancy Activation Energies

Nuclear magnetic resonance studies on pure solid He^4 and on He^3 impurity probes in solid He^4 have demonstrated that at elevated temperatures there is an activation energy ϕ to create a vacancy. If this were the only energy in the problem the fraction of vacant sites (x) would vanish as $T \to 0$. In order to achieve a finite vacancy concentration at absolute zero, we require an energy function which has a minimum at $x = x_o \neq 0$. Suppose that the vacancies have an energy of mutual attraction as well as an energy of creation. Then the vacancy energy per site (normalized to zero as $x \to 0$) might be parametrized (for example) as

$$\Delta\varepsilon(x) = \phi x - u_{att}\, x^{(1-\beta)} + \ldots \qquad (3.1a)$$

$$0 < \beta < 1 \qquad (3.1b)$$

where u_{att} is a parameter describing the overall strength of mutual attraction. We have no theoretical justification for this expression other than the fact that equation 3.1 leads to thermally activated vacancies at elevated temperatures and Bose-Einstein vacancy condensation at lower temperatures. However, the final results, such as the

critical temperature, depend only on the position of the minimum and not on the details of the interaction.

The total energy to add one vacancy to the crystal (at T=0), given a concentration x already present is

$$\overline{\phi} = (\partial \Delta\varepsilon/\partial x) \quad . \tag{3.2}$$

This can be written

$$\overline{\phi}(x) = \phi[1-(x_o/x)^{\beta}] \quad (x \geq x_o) \tag{3.3}$$

where x_o is the ground state concentration which minimizes $\Delta\varepsilon(x)$. We note the following properties. For $x >> x_o$, $\overline{\phi}(x) = \phi$, a constant, as observed in nuclear magnetic resonance (NMR) studies at elevated temperatures. As the temperature drops $x \to x_o$. NMR quantities become temperature independent below about 1 °K. The usual interpretation is that relaxation processes are due to particle exchange (i.e., J_{34}, J_{33}) although temperature independence is also consistent with $x \to x_o$. In any case an upper limit to x_o has been estimated (10) from the data to be $x_o \lesssim 10^{-4}$. We have not succeeded in calculating x_o from energy considerations. However, using a Feynman model wave function below, we are able to make a quantitative estimate of x_o.

The Feynman Model State for He^4

The first reasonable quantitative estimate of the Bose condensate order parameter in strongly interacting systems was made by Penrose and Onsager (5) using a simple wave function proposed by Feynman. The wave function is assumed constant in regions of configuration

space where all pairs of helium atoms are separated by more than an effective hard core diameter σ. If any two helium atoms are separated by a distance less than σ then the wave function vanishes. Formally the spatial configurations of the helium atoms in the Feynman model state are identical to those of classical rigid spheres in thermal equilibrium at arbitrary temperature. This can be seen as follows. The Feynman wave function ψ is

$$\psi(\underset{\sim}{r}_1 \cdots \underset{\sim}{r}_N) = \Omega_N^{-\frac{1}{2}} F_N(\underset{\sim}{r}_1 \cdots \underset{\sim}{r}_N) \quad , \qquad (3.4)$$

where Ω_N is a normalizing constant and $F_N(x_1 \cdots x_n)$ is equal to one when no hard spheres overlap and zero if they do. In terms of the normalizing constant, the configurational partition function for N hard spheres is $\Omega_N/N!$ The probability of a particular configuration $(r_1 \cdots r_N)$ is $N![\psi(r_1 \cdots r_N)]^2$ which is equal to $N!/\Omega_N$ if no spheres overlap or zero if they do. However this is identical to the probability of a particular configuration for classical hard spheres at arbitrary temperature. Thus any quantity depending on the distribution of particles can be found by calculating that quantity in the classical hard sphere model. For example the vacancy concentration in the solid phase and the volumes of melting and crystallization will be identical for classical hard spheres and the Feynman wave function approximation.

Since our quantitative predictions are based on the Feynman model wave function, it is important to discuss which physical quantities can be calculated at all reliably from this simple data. It is evident that this model wave function is most inadequate when calculating the

energy and derivatives such as pressure, sound velocity, etc. The wave function has an unphysical discontinuous change as two atoms overlap which corresponds to an infinite kinetic energy. However, if the wave function has meaning for He^4 we should be able to calculate quantities which depend on the distribution of particles. It will be seen that with an appropriate choice of σ there is excellent agreement between this simple theory and experiment.

We first consider short range correlations. Naturally the theoretical radial distribution function cannot agree with experiment near the hard-core diameter since the function in the model changes discontinuously from the first peak to zero at the hard-core diameter. Penrose and Onsager (5) take the effective hard-core diameter to be $\sigma \cong 2.6$ Å, the diameter of a He^4 atom. However, by choosing the hard core diameter to be at the first peak in the liquid helium radial distribution function ($\sigma \cong 3.34$ Å) (26) excellent agreement is obtained with the next few peaks as shown by recent experiments by Bernal and King (27). By shaking a number of spheres in a bag to form random arrangements, they find that the second, third and fourth peaks are accurately predicted with $\sigma = 3.34$ Å as seen in Table I. Their results in units of $\sigma = 3.34$ Å are given along with the experimental results for liquid He^4.

Table I. Peaks in radial distribution function.

	Second	Third	Fourth
Bernal and King results	1.8(3)	2.6(4)	3.5(8)
Liquid He^4	1.8(7)	2.6(6)	3.4(5)

The apparent improvements in the model with a larger σ in predicting short range correlations is even more striking when we consider long range ordering as a function of v, the volume per atom. Computer calculations (28) for hard core correlations indicate a phase transition, at arbitrary temperature, from a gas to a HCP solid at the following volumes of crystallization (v_c) and melting (v_m):

$$v_c = 23.4 \text{ cm}^3/\text{mole} , \tag{3.5a}$$

$$v_m = 21.1 \text{ cm}^3/\text{mole} . \tag{3.5b}$$

The corresponding experimental volumes for He^4 are for T = 0-1 °K independent of temperature and given by (29):

$$v_c = 23.3 \text{ cm}^3/\text{mole} , \tag{3.6a}$$

$$v_m = 21.2 \text{ cm}^3/\text{mole} . \tag{3.6b}$$

It is evident that the Feynman wave function is capable of describing (with σ = 3.34 Å) the change in the long range order associated with freezing and melting. Our hope is that the model does just as well in describing the long range order associated with Bose-Einstein condensation and vacancy formation.

The Ground State Order Parameter

We define the ground state order parameter in the following manner. For a normalized many Boson wave function the reduced one particle density matrix is

$$\rho(\underset{\sim}{r},\underset{\sim}{r}') = N \int_{\Omega} d^3r_1 \cdots \int_{\Omega} d^3r_{N-1} \, \psi^*(\underset{\sim}{r}_1 \cdots r_{N-1}\underset{\sim}{r}') \, \psi(\underset{\sim}{r}_1 \cdots \underset{\sim}{r}_{N-1},\underset{\sim}{r}) \quad . \tag{3.7}$$

By definition, the ground state order parameter is that fraction of He^4 atoms having zero momentum.

$$\xi = \lim_{\Omega\to\infty} \left[\frac{v}{\Omega^2} \int d^3r \int d^3r' \, \rho(\underset{\sim}{r},\underset{\sim}{r}')\right] \tag{3.8}$$

where v is the volume per particle and Ω is the total volume. For the liquid ξ, the Bose condensate fraction, is finite in the superfluid phase but drops to zero at the λ-transition.

For liquid He^4 Penrose and Onsager (5) have shown that $\xi = 1/vz$ where $z = (N+1)\Omega_N/\Omega_{N+1}$ is the activity [$z = \ell n(\mu)$ where μ is the chemical potential] of a hard core system. Using the Feynman wave function the integral in equation 3.7 is now related to the pair distribution function $n_2(r,r')$ for N+1 hard spheres where $n_2(r,r')$ is defined by

$$n_2(\underset{\sim}{r},\underset{\sim}{r}') \equiv [(N+1)(N)/\Omega_{N+1}] \int d^3\underset{\sim}{r}_1 \cdots \int d^3r_{N-1} \, F_{N+1}(\underset{\sim}{r}_1 \cdots \underset{\sim}{r}_{N-1},\underset{\sim}{r},\underset{\sim}{r}') \tag{3.9}$$

Using equations 3.7 and 3.9 we see that

$$\rho(\underset{\sim}{r},\underset{\sim}{r}') = Z^{-1} \, n_2(\underset{\sim}{r},\underset{\sim}{r}') \tag{3.10}$$

when $|r-r'| \geq \sigma$. For $|r-r'|$ large $n_2(r,r') = (N/V)^2$. In this case the density matrix $\rho(r,r')$ is given by

$$\lim_{(r-r')\to\infty} \rho(\underset{\sim}{r},\underset{\sim}{r}') \cong Z^{-1}(N/\Omega)^2 \quad . \tag{3.11}$$

Inserting this expression in equation 3.7 yields

$$\xi = \frac{v}{z}(N/\Omega)^2 = \frac{1}{vz} \quad . \tag{3.12}$$

For the solid $\rho(r,r')$ has the periodicity of the lattice and is probably not constant. Penrose and Onsager (5) point out that for a solid if x=0 then $\rho(r,r')$ is only appreciable if r and r' are near the one remaining lattice site since all other sites are filled in the absence of vacancies. However, as we shall see, there are ground state vacancies in a classical hard core system. In this case $\rho(\underset{\sim}{r},\underset{\sim}{r}') \neq 0$ $|\underset{\sim}{r}-\underset{\sim}{r}'| >> 0$ because an itinerant vacancy has a finite amplitude to be at any crystal site and therefore there is a long range correlation in $\rho(\underset{\sim}{r},\underset{\sim}{r}')$. For large $|\underset{\sim}{r}-\underset{\sim}{r}'|$ we then expect that the average value [the averaging procedure removes the periodic variation in $\rho(\underset{\sim}{r},\underset{\sim}{r}')$] of ρ to be given by equation 3.11 with $\xi = 1/vz$ as in the liquid.

We calculate ξ using the hard core expansions of de Llano and Ramirez (28) quoted below. For a system of N hard spheres of mass m the classical expression for the Helmholtz free energy A at temperature T is given by

$$A = -kT \ln (\Omega_N/N!\ \lambda^{3N}) \tag{3.13}$$

where the thermal wavelength $\lambda = \sqrt{2\pi\hbar^2/mkT}$. We define

$$\alpha(y) \equiv A/NkT - \ln(\lambda^3\rho_o) = -\ln [\frac{1}{y} - b(y)] - 1 \tag{3.14}$$

with $y = \rho/\rho_o$, and $b(y) = b(\rho)/\rho_o$, where ρ is the density and $b(\rho)$ is the density dependent but unknown average excluded volume per particle. ρ_o is the close packing density equal to $\sqrt{2}/\sigma^3$ for the HCP lattice.

The activity is calculated as follows. From equation 3.13 and the definition of z we find

$$z = \exp\{[A(N+1,V,T)-A(N,V,T)]kT - \ell n\ \lambda^3\} \quad . \tag{3.15}$$

Using equation 3.14 this becomes

$$z = \exp\{(N+1)\ \alpha[y(\tfrac{N+1}{N})] - N\ \alpha(y) + \ell n\ \rho_o\} \quad , \tag{3.16a}$$

or

$$z \cong \rho_o \exp\ [\alpha(y) + y\ \alpha'(y)] \quad . \tag{3.16b}$$

The prime means to differentiate with respect to y. Using $P = -(\partial A/\partial V)_T$ we can define a reduced pressure

$$\pi(y) \equiv P/\rho_o\ kT = y^2\ \alpha'(y) = \frac{y + y^3\ b'(y)}{1 - y\ b(y)} \quad . \tag{3.17}$$

The condensate fraction is then given by

$$\xi = y \exp -[\alpha(y) + \pi(y)/y] \quad . \tag{3.18}$$

The result derived from the Carnahan-Starling equation of state in reference (28) was used to approximate b(y) in the fluid. The result is

$$y\ b(y) = 1 - \exp -\left[\frac{(2\pi\sqrt{2}/3)y - (\pi^2/6)y^2}{[1-(\pi\sqrt{2}/6)\ y\ ]^2}\right] \quad . \tag{3.19}$$

For the solid we used the asymptotic expansions about close packing of Salzburg et al. (30):

$$\alpha(y) = -3\ \ell n(1/y - 1) + 1.7795 - \ell n\ (\rho_o\sigma^3) + .557994\ (1/y - 1) \quad . \tag{3.20}$$

The reduced pressure in this approximation is given by

$$\pi(y) = 3y/(1-y) - .557994 \quad . \tag{3.21}$$

These expressions give good agreement with the Monte Carlo calculations of the gas to solid phase transition by Hoover and Ree (31). There is no liquid phase since there is no attractive part of the potential in this model. The results for the condensate fraction (32) are given in figure 10. These results are very sensitive to the value of σ used. For the value $\sigma = 2.6$ Å used by Penrose and Onsager (5) the condensate fraction at $v = 27$ cm^3/mole is 8% rather than $\sim 10^{-5}$ as given here.

The Ground State Vacancy Concentration

The fraction of ground state vacancies in the Feynman-Penrose-Onsager model is identical to the fraction of vacancies in a classical hard core solid at arbitrary temperature. This can be computed by estimating the classical activation free energy to form a vacancy. The reader must be warned that the activation energies discussed in this section are not the activation energies for the physical He^4 crystal.

In the classical hard-core solid we can easily estimate the work done to create a vacancy. In allowed regions of phase space (not excluded by the hard core), the potential energy of the classical solid is zero. The work required to "hollow out a hole" in the crystal is then pv_{eff}, where v_{eff} is the empty volume around a given site required for the existence of a physical vacancy. This will be somewhat less than the volume per particle v since the neighboring atoms to a vacancy

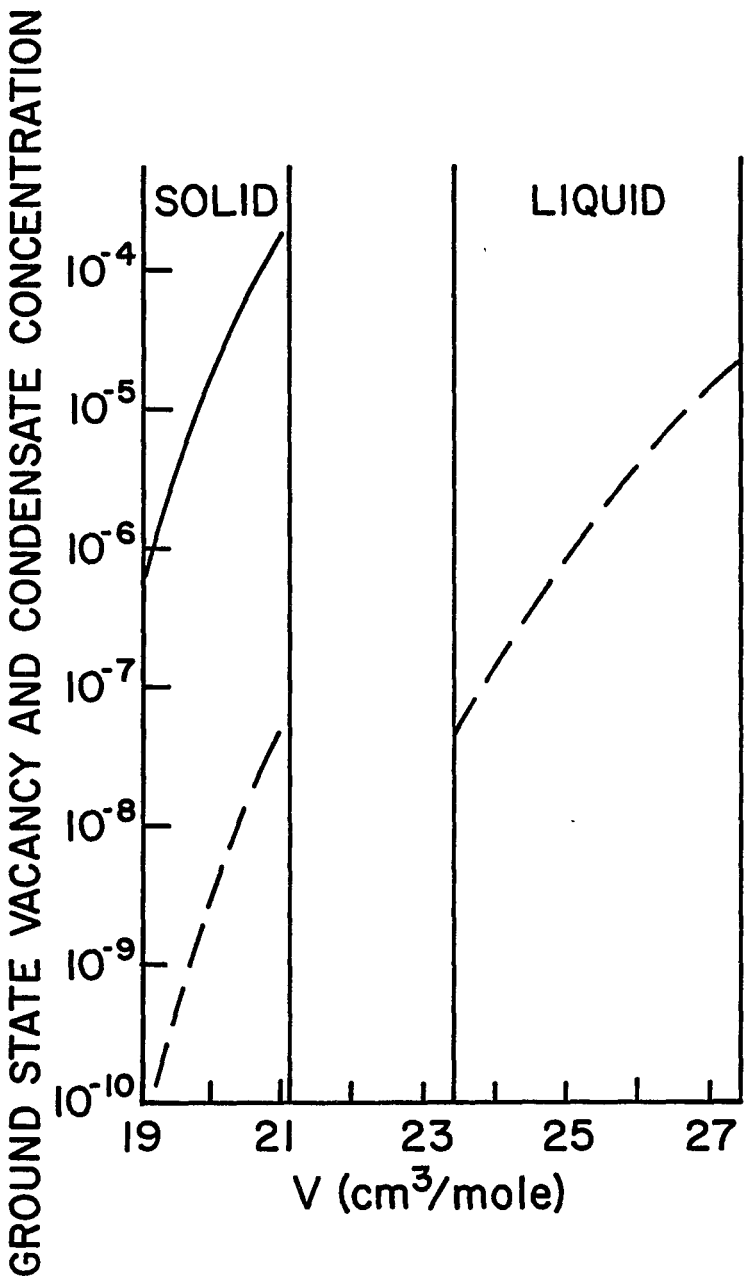

Fig. 10. The ground state vacancy concentration (solid line) and the Bose condensate fraction (dotted lines) plotted as functions of the volume.

will generally be off their equilibrium sites, i.e., pushed closer to the vacancy site. We estimate $v_{eff} = \sigma^3/\sqrt{2}$, the volume per particle at closest packing. The Boltzmann factor for the number of vacancies is then

$$x_o \simeq \exp -(p\sigma^2/kT\sqrt{2}) = e^{-\pi(y)} \quad . \tag{3.22}$$

The vacancy concentration is independent of temperature in this model.

We note that the hard core classical solid is in some ways a poor approximation to the real solid. For example, the pressure goes to zero at T=0 unlike the real solid where p = 25 atmospheres. We also know that the number of vacancies increases with temperature in the real solid above 1 °K. However, in view of our previous discussion of the Feynmann wave function, it is reasonable to believe that the ground state vacancy concentration is correctly predicted by equation 3.22. Our predicted values for the ground state vacancy concentration x_o are plotted as a function of volume in figure 10.

Statistical Thermodynamics of Vacancies

The statistical mechanics of the solid He^4 crystal with a concentration of x vacancies per site is determined by the Helmholtz free energy A(T,v,x) via

$$dA = -sdT - pdv + \xi dx \quad . \tag{3.23}$$

The equilibrium concentration of vacancies is that which minimizes A(T,v,x); hence,

$$\xi = 0 \ , \quad \begin{matrix}\text{(physical value of the} \\ \text{vacancy chemical potential)}\end{matrix} \quad . \tag{3.24}$$

For formal purposes, it is convenient to consider arbitrary values of ξ.

From the work of Andreev and Lifshitz (1) it is evidence that vacancies in a Boson quantum crystal will propagate in Bloch energy bands. In zeroth order, the vacancy is localized at a site in a Wannier state. However, the nearest neighbor tunneling matrix element t broadens the localized states into mobile solid state bands in the usual manner. Since the HCP crystal has two sites per unit cell, there will be two vacancy bands:

$$E = E_{\gamma}(\underset{\sim}{k}); \quad \gamma = 1,2 \quad . \tag{3.25}$$

These can be normalized to zero energy at the minimum of the lowest band. Let A_o be the free energy per lattice site of an ideal Bose gas of vacancies with the spectra in equation 3.25. The total free energy per lattice site is then (in mean field theory)

$$A = A_o + \Delta\varepsilon \quad , \tag{3.26}$$

where $\Delta\varepsilon$ has been defined in the first section of this chapter. Differentiating equation 3.26 with respect to x yields, from equations 3.2 and 3.14,

$$\xi = \xi_o + \overline{\phi} \quad , \tag{3.27}$$

where ξ_o can be calculated via the usual ideal Bose gas rule

$$x = \frac{1}{N} \sum_{\gamma} \sum_{\underset{\sim}{k}} f[E_{\gamma}(\underset{\sim}{k}) - \xi_o] \quad , \tag{3.28}$$

$$f(E) = [e^{E/kT} - 1]^{-1} \quad . \tag{3.29}$$

The "self-consistent" equation for calculating the equilibrium vacancy concentration at temperature T follows from equations 3.24, 3.27 and 3.28. It is, in the thermodynamic limit (32),

$$x = v \sum_{\gamma} \int \frac{d^3k}{(2\pi)^3} f[E_{\gamma}(\underset{\sim}{k}) + \bar{\phi}(x)], \quad x \geq x_o \quad . \tag{3.30}$$

In the high temperature limit $x >> x_o$, $\bar{\phi}(x) \cong \phi$ and

$$x \cong e^{-\phi/kT} [v \sum_{\gamma} \int \frac{d^3k}{(2\pi)^3} [e^{E_{\gamma}(\underset{\sim}{k})/kT} - 1]^{-1} \quad . \tag{3.31}$$

The vacancies behave as thermally activated Boltzmann particles. As $T \to T_c^+$, the vacancy concentration quickly decreases to x_o (the ground state concentration). The precise way this occurs depends on the $\bar{\phi}(x)$ function, e.g., the value of β in equation 3.3. The transition temperature is characterized by $x(T) \to x_o$ as $T \to T_c^+$. Using this criterion for the definition of T_c we find

$$x_o = v \sum_{\gamma} \int \frac{d^3k}{(2\pi)^3} [e^{E_{\gamma}(\underset{\sim}{k})/kT_c} - 1]^{-1} \tag{3.32}$$

as our fundamental equation for calculating the transition temperature T_c. It should be noted that this result does not depend on our detailed parametrization of the $\overline{\phi}(x)$ function.

To calculate T_c, the appropriate energy levels $E_\gamma(\underset{\sim}{k})$ for a HCP lattice must be inserted in equation 3.32. For the HCP crystal the lattice basis vectors are $a_1 = (\Delta,0,0)$; $a_2 = (\frac{1}{2}\Delta, \frac{\sqrt{3}\Delta}{2}, 0)$; and $a_3 = (0, 0, 8/3\ \Delta)$. The energy bands in a tight binding approximation are given by (22)

$$E_\gamma(\underset{\sim}{k}) = -2t\ \{\cos\ (\underset{\sim}{k}\cdot\underset{\sim}{a}_1) + \cos\ (\underset{\sim}{k}\cdot\underset{\sim}{a}_2) + \cos\ [\underset{\sim}{k}\cdot(\underset{\sim}{a}_1-\underset{\sim}{a}_2)]\}$$

$$\pm\ 2t\ \cos\ \frac{\underset{\sim}{k}\cdot\underset{\sim}{a}_3}{2}\ \left\{3 + 2\{\cos\ \underset{\sim}{k}\cdot\underset{\sim}{a}_1 + \cos\ \underset{\sim}{k}\cdot\underset{\sim}{a}_2 + \cos\ [\underset{\sim}{k}\cdot(\underset{\sim}{a}_1-\underset{\sim}{a}_2)]\}\right\}^{\frac{1}{2}}. \tag{3.33}$$

For temperatures $T \sim T_c$, the thermal energy $k_B T$ is much less than the bandwidth and we may assume that only states with small k in the lower band are important. Expanding the lower energy band of equation 3.33 to second order in $\underset{\sim}{k}$ we find

$$E(\underset{\sim}{k}) \cong -12t + 2t\ \Delta^2(\underset{\sim}{k})^2 \quad . \tag{3.34}$$

Except for the constant energy shift (-12t) the above expression looks like a free particle dispersion relation [$E(\underset{\sim}{k}) = \hbar^2\underset{\sim}{k}^2/2m^*$] with an effective mass $m^* = \hbar^2/4t^2$.

The critical temperature may now be calculated assuming that we have a dilute gas of bosons with mass m*. Inserting $E(\underset{\sim}{k}) = \hbar^2\underset{\sim}{k}^2/2m^*$ in equation 3.32 and performing the integral yields

$$\frac{x_o\lambda^3}{v} = \sum_{s=1}^{\infty} s^{-3/2} \; ; \quad \lambda = \left(\frac{2\pi\hbar^2}{m^*kT}\right)^{\frac{1}{2}} \quad . \tag{3.35}$$

We then find

$$T_c = 16.7(t/k)\, x_o^{2/3} \quad . \tag{3.36}$$

Using the experimental pressure as a function of volume (18) and equations 3.22 and 3.36, we plot the λ-line in the solid phase. The result is shown in figure 11. We recall from the third section in Chapter 2 that $t \sim 0.1$ °K. With $x_o \cong 10^{-4}$ at melting we have $T_c \sim 10^{-2}$ °K.

Conclusions

We have argued that ground state vacancies may exist in solid He^4 and that Bose condensation of these vacancies will cause a phase transition on the melting curve of the solid at $T_c \sim 10^{-2}$ °K. For pressures higher than the melting pressure the critical temperature rapidly decreases as shown in figure 11. We discuss how this transition could in principle be detected along with a more practical possibility of detecting ground state vacancies at more accessible temperatures (32).

The λ-transition will be accompanied by a specific heat anomaly, but the integrated strength (the entropy change) will be $\sim k_B x_o \ln(e/x_o)$

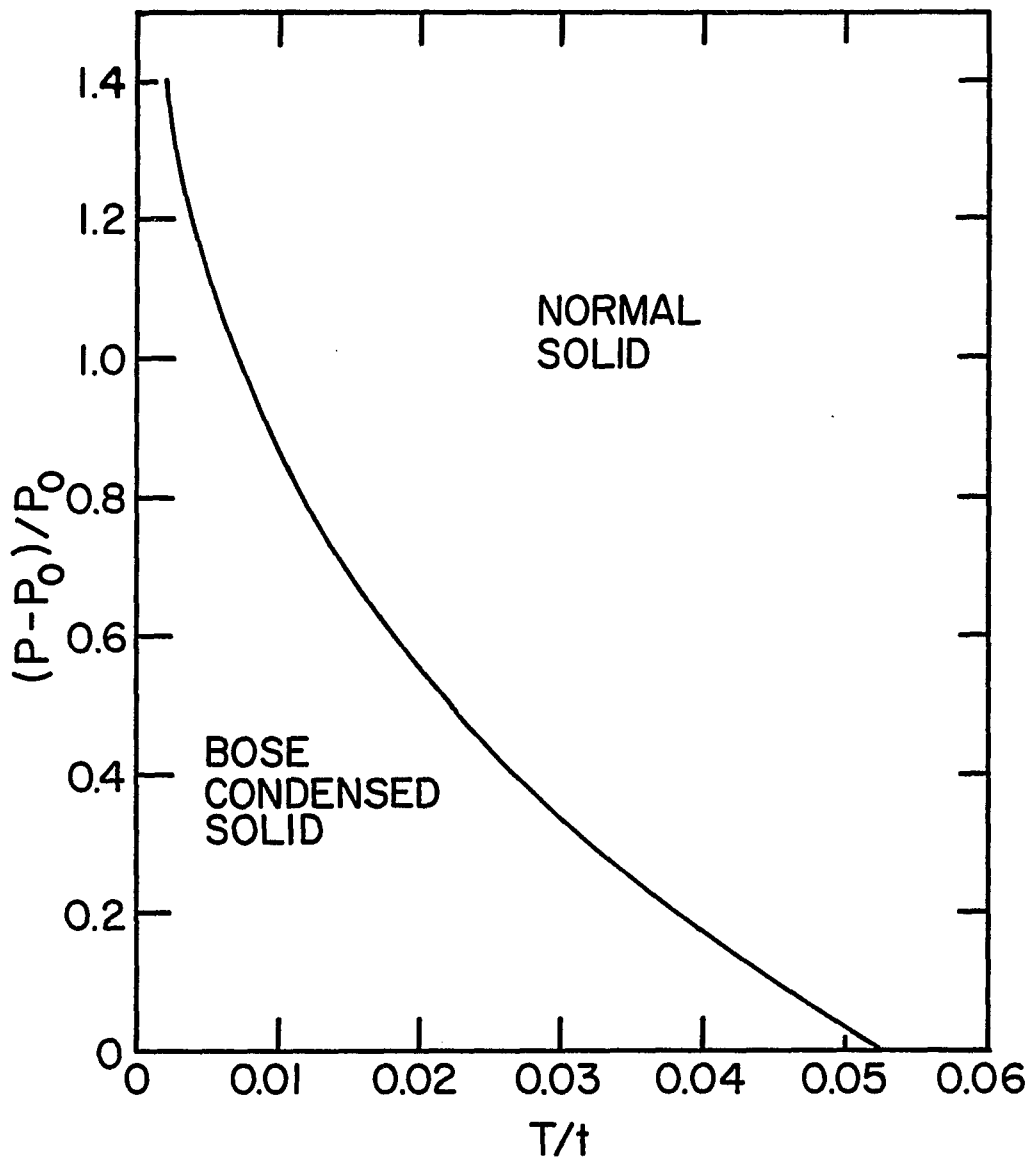

Fig. 11. The Bose condensed phase in the solid is shown on a $(P-P_o)/P_o$ vs. T diagram.

T is in units of the vacancy hopping parameter t and P_o is the pressure at melting.

which is probably too small to be observed. On the other hand, it appears probable that the transition will also be accompanied by some form of superfluidity in the solid phase. The vacancies form an almost ideal Bose gas within the inert solid background. Vacancy transport in a given direction corresponds to physical mass transport in the opposite direction. Thus, the vacancy superfluidity implies crystal superfluidity. The mass transported by a vacancy is of the order of one He^4 atomic mass; hence the maximum superfluid density fraction $(\rho_s/\rho)_{max} \sim x_o << 1$. Nevertheless, for $T < T_c$ it should be possible to have a superleak in a vessel containing the solid phase.

Consider the following thought experiment. Suppose that two vessels containing solid He^4 are connected by a narrow channel capillary. One of the vessels has a higher pressure with a correspondingly smaller vacancy concentration than the other vessel. For $T < T_c$, the vacancies will flow in a superfluid manner through the channel until the pressure and vacancy concentration is equalized in each vessel. One then has obtained a situation where mass flows without viscosity through a narrow capillary connecting two vessels containing solid He^4. The transition at $T = T_c$ could be detected by monitoring the sudden relaxation of a physical pressure difference as the temperature is lowered from above T_c. The problem with the above experiment is that such a low temperature is presently experimentally inaccessible for ultrapure He^4.

We now attempt to show that the presence of ground state vacancies may also be demonstrable in view of the results of the

sixth section of Chapter 2. For $x_o \sim 10^{-4}$ the diffusion is dominated by He^3-vacancy molecules. Using equation 2.24 we have approximately

$$D = \frac{\pi n_b x_o t' \Delta^2}{4\hbar x_3 \sigma^*} \tag{3.37}$$

with $\sigma^* \sim 10$. For $n_b = 12$, $x_o \sim 10^{-4}$ and $t' \sim 10^{-2}$ °K this result agrees with experiment (23). As the temperature is lowered to $k_B T \sim E_{binding}$, the diffusion should increase due to the increase in occupancy of molecular states. Therefore if the diffusion increases as the temperature is lowered below ~ 0.1 °K the presence of ground state vacancies will be clearly indicated.

CHAPTER 4

CONSEQUENCES OF THE IMPURITON-IMPURITON MOLECULE IN SOLID He^4

In this chapter we will consider a model system (33) in which vacancies are not present but a small concentration of He^3 impurities are present in an otherwise pure He^4 crystal, i.e., there are no ground state vacancies and the temperature of the crystal is sufficiently low that we may ignore thermally excited vacancies. We will consider whether NMR data are adequately explained with a model which involves only the He^3-He^3 exchange parameter J_{33} and the He^3-He^4 exchange parameter J_{34}. If ground state vacancies exist, the only change in this chapter would be to attribute the diffusion to impuriton-vacancy molecules as was done in Chapter 3 rather than impuriton motion as we do in this chapter.

Impuriton-Impuriton Molecular Energy Bands and Crystal Structure Effects

If $J_{33} >> J_{34}$, as has been reported (2), hopping induced two impuriton bound states, of the type analyzed in Chapter 2, will be formed. We will show that these states have great importance for the interpretation of the experimental NMR data. Experiments are generally performed on the HCP phase of solid He^4; therefore, we first consider what modifications of the results obtained for a cubic lattice must be made for a HCP lattice.

We first consider the limit $J_{34} = 0$ and J_{33} finite. In any lattice the spectrum is as shown in figure 12. The separated atoms have energy E=0. The z-fold degenerate triplet states are at $E = J_{33}$, where z is the number of nearest neighbors (12 for HCP). The z-fold degenerate singlet molecular states are at $E = -J_{33}$. When J_{34} is turned on the separated atoms are split into scattering states of bandwidth $4zJ_{34}$. In a HCP structure the molecular states are split into rotational or waddling bands as shown in figure 13. In this structure the molecule can move by a first order process since either atom can hop from a nearest neighbor to a nearest neighbor of the other. However, in a cubic crystal this process is second order since one atom must first hop away from the other for the molecule to move. This process would then occur with an amplitude $\sim J_{34}^2/J_{33}$ since J_{33} is the energy difference in the intermediate state. The bandwidth is then $\sim zJ_{34}^2/J_{33}$. We see therefore that the molecular bandwidth goes to zero for $J_{33} >> J_{34}$ in a cubic crystal but not in a HCP crystal where it is zJ_{34} in this limit.

Looking at figure 6 we note that the molecular bands are not centered at J_{33} but are repelled by the scattering band to a somewhat greater value. We do not know how big this effect would be in a HCP lattice since this structure has only been solved (22) in the limit $J_{33} >> J_{34}$. We conjecture that the repulsion is bigger in the HCP since molecules should be easier to form. The value for the mean energy of the molecular band relative to the mean energy of the scattering band, (Ω_m) which fits the experimental results is $\Omega_m \approx 5J_{33}$.

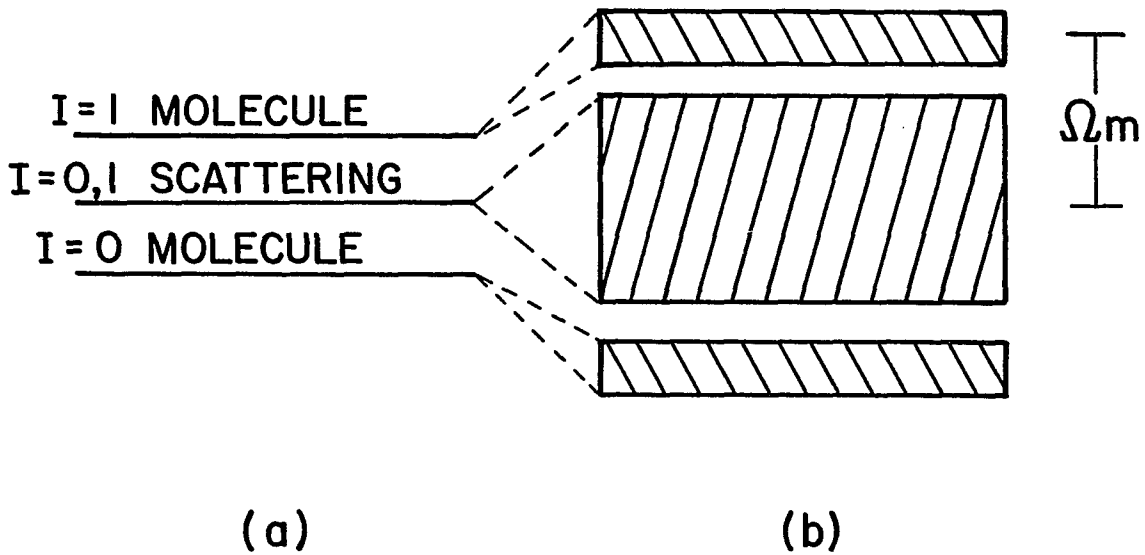

Fig. 12. Schematic illustration of energy levels of He^3-He^3 molecular energy bands.

In part (a) the parameter $J_{34} = 0$ and the energy level structure is that of a stationary molecule. In part (b) $J_{34} \neq 0$ and the He^3 atoms may now migrate. The stationary molecule levels are now spread into bands.

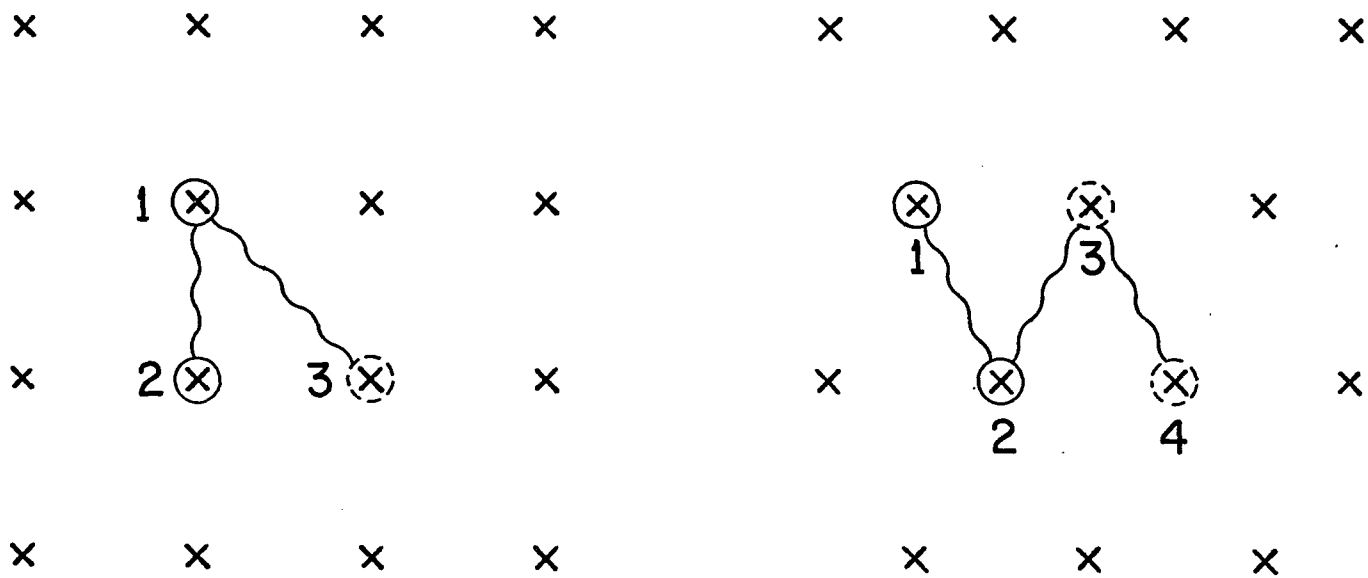

Fig. 13. Illustration of the effect of lattice structure on the hopping amplitude of He^3-He^3 molecules.

In the square lattice a molecule at sites 1 and 2 can move only by processes which break it apart such as the atom at 2 moving to site 3. In the triangular lattice the molecule can move without breaking apart such as by 1 going to 3, then 2 going to 4, etc. A tightly bound molecule cannot move in the first case, but can in the second. Cubic and BCC lattices are of the first type, HCP of the second.

In figure 14 we show the band structure of the triplet state He^3-He^3 molecules for a HCP lattice along certain symmetry lines in the Brillouin zone shown in figure 15. The degeneracy of the states is also shown. This band structure was obtained by Sacco and Widom (22) in the limit $J_{33}/J_{34} \to \infty$.

Theory of Spin Diffusion

The theory of impuriton motion based on spin diffusion data has been mentioned in Chapter 1. While the $1/x_3$ dependence of the diffusion constant indicated gas-like motion of the He^3 impurities, the details of the calculation deriving this result lead to a contradiction. In their attempt to quantitatively account for the He^3 diffusion data, Richards, Pope and Widom (2) assumed that $R \cong \Delta$ (equation 1.3). They then found that it was necessary to take $J_{33} \sim 10^2$-10^3 J_{34} in order to obtain a good fit to the data. This result was regarded as unacceptable since the mass difference makes J_{34} smaller, but not 2 to 3 orders of mangitude smaller, than J_{33}. However it now appears for two reasons that J_{34} is not anomalously small as the above calculation (2) suggests.

At the time of the initial data analysis J_{33} had been incorrectly calculated from specific heat data on solid He^3. It was found from an analysis of other data that He^4 impurity motion had made an unexpectedly large contribution to the specific heat (18). J_{33} is now considered to be a factor of four less than previously assumed. A second and more important effect is that if $J_{33} >> J_{34}$ there will be a number of bound states formed which markedly increase the He^3-He^3 scattering cross section. In view of this, we have recalculated the

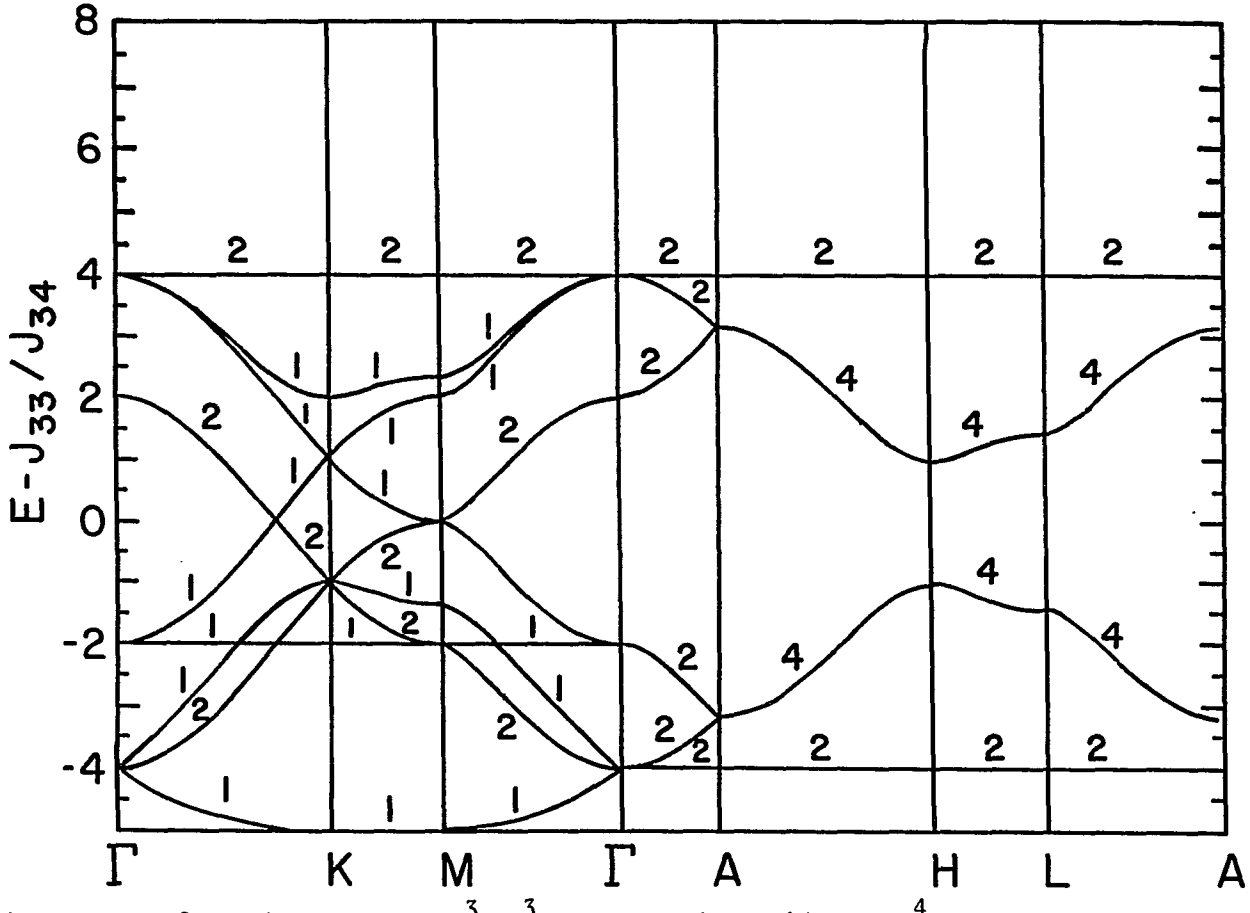

Fig. 14. Band structure for triplet state He^3-He^3 molecules in solid HCP He^4.

The degeneracy of each state is given by the numbers in the figure. The band structure was obtained in the limit $J_{33}/J_{34} \to \infty$.

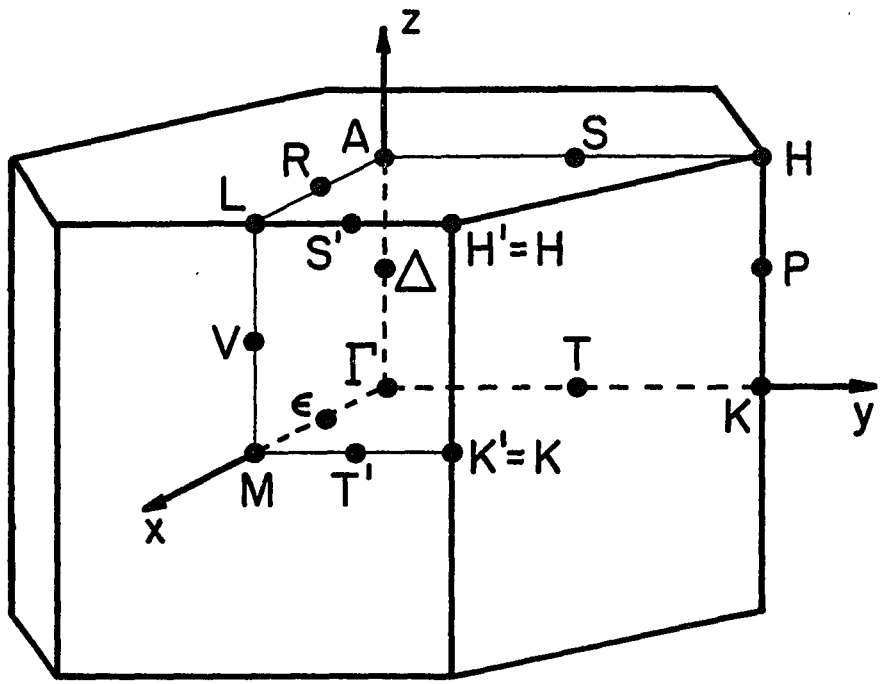

Fig. 15. The Brillouin zone of the HCP crystal.

He^3 diffusion constant in a self consistent way that properly includes the effects of bound states. The details are given in Appendix B. The result of this analysis is that

$$D = \frac{\pi}{8\hbar} \frac{J_{34} \Delta^2}{\sigma^* x_3} \tag{4.1}$$

where

$$\sigma^* = 2 \overline{\sum_\alpha g_\alpha \sin^2 \delta_\alpha} \tag{4.2}$$

σ^* is a dimensionless cross section, δ_α is the phase shift in a particular crystal group representation α, and g_α is the degeneracy of that representation. The bar means to average over all energy states. We argue in Appendix B that σ^* is approximately equal to the number of bound triplet or singlet molecular states. Thus $\sigma^* \cong 12$ for the HCP lattice.

Experimentally, for He^3 concentrations between 10^{-2} and 10^{-4}, the diffusion constant is given by

$$D = D_o/x_3 \tag{4.3}$$

where $D_o = 1.2 \times 10^{-11}$ cm^2/sec at a volume of 21 $cm^3/mole$ with $\Delta =$ 3.67 Å. Under the previous hard core assumption $\sigma^* \cong 1$, the anomalously small result $J_{34}/\hbar \cong 4 \times 10^4/sec$ was obtained. With $\sigma^* \cong 12$, we find $J_{34}/\hbar \cong 4 \times 10^5/sec$. J_{33} can be estimated by extrapolating its value in solid He^3 in the HCP phase to the same volume giving $J_{33}/\hbar \cong$ $4 \times 10^6/sec$.

Our result of $J_{34}/\hbar \cong 4 \times 10^5$/sec is still a factor of 10 smaller than the estimated J_{33}. (The He^3-He^4 mass difference could easily account for part of this difference.) More importantly, we have assumed J_{33} was large enough to produce all 24 bound states. Our result is therefore self consistent in the sense that those bound states would still be expected to exist for $J_{33} \cong 10\ J_{34}$ and not disappear into the band.

Theory of the Nuclear Magnetic Resonance T_1 Including the Effects of He^3-He^3 Molecules

The NMR relaxation time $T_1(\Omega_o)$ is the decay time of the z component of the magnetization in a magnetic field H_o ($\Omega_o = \gamma H_o$ where $\gamma = 2.04 \times 10^4$ rad/G·sec for He^3). To calculate $T_1(\Omega_o)$ we have to consider the dipole-dipole interaction inducing transitions between states with different z components of spin. Classically (34) the interaction is given by

$$V_{ij} = \left(\frac{\mu_i \cdot \mu_j}{r_{ij}^3}\right) - \frac{3(\mu_i \cdot r_{ij})(\mu_j \cdot r_{ij})}{r_{ij}^5} \quad . \tag{4.5}$$

with $\mu_i(\mu_j)$ the magnetic moment of the i^{th} (j^{th}) nucleus. Writing $\mu = \gamma\hbar I$ the expression for a system of identical magnetic dipoles when summed over all neighbors is

$$V_{ij} = \gamma^2\hbar^2\, r_{ij}^{-3}\, [(I_i \cdot I_j) - 3(I_i \cdot p_{ij})(I_j \cdot p_{ij})] \quad , \tag{4.6}$$

where p_{ij} is a unit vector parallel to r_{ij}. In terms of unit vectors λ_1, λ_2, and λ_3 parallel to Cartesian axes x, y, and z, we write

$$I_i = \lambda_1 I_{x_i} + \lambda_2 I_{y_i} + \lambda_3 I_{z_i} \quad , \tag{4.7}$$

and

$$p_{ij} = \lambda_1 \varepsilon_1 + \lambda_2 \varepsilon_2 + \lambda_3 \varepsilon_3 \quad , \tag{4.8}$$

where ε_1, ε_2 and ε_3 are direction cosines. Then

$$\begin{aligned} V_{ij} = \gamma^2\hbar^2 r_{ij}^{-3} [& I_{x_i} I_{x_j} (1-3\varepsilon_1^2) + I_{y_i} I_{y_j} (1-3\varepsilon_2^2) + I_{z_i} I_{z_j} (1-3\varepsilon_3^2) \\ & -3(I_{x_i} I_{y_j} + I_{x_j} I_{y_i})\varepsilon_1\varepsilon_2 - 3(I_{y_i} I_{z_j} + I_{y_j} I_{z_i})\varepsilon_2\varepsilon_3 \\ & -3(I_{z_i} I_{x_j} + I_{z_j} I_{x_i})\varepsilon_3\varepsilon_1] \quad . \end{aligned} \tag{4.9}$$

In terms of spherical polar coordinates, the direction cosines are

$$\begin{aligned} \varepsilon_1 &= \sin\theta_{ij} \cos\phi_{ij} \quad , \\ \varepsilon_2 &= \sin\theta_{ij} \sin\phi_{ij} \quad , \\ \varepsilon_3 &= \cos\theta_{ij} \quad . \end{aligned} \tag{4.10}$$

Substituting equation 4.10 into 4.9 we find

$$V_{ij} = \gamma^2\hbar^2 r_{ij}^{-3} (A+B+C+D+E+F) \quad , \tag{4.11}$$

where

$$A = I_{z_i} I_{z_j} (1 - 3 \cos^2 \theta_{ij}) \quad ,$$

$$B = -\frac{1}{4}[(I_{x_i} - iI_{y_i})(I_{x_j} + iI_{y_j}) + (I_{x_i} + iI_{y_i})(I_{x_j} - iI_{y_j})] (1 - 3 \cos^2 \theta_{ij}),$$

$$C = -\frac{3}{2}[(I_{x_i} + iI_{y_i})I_{x_j} + (I_{x_j} + iI_{y_j})I_{z_i}] \sin \theta_{ij} \cos \theta_{ij} \exp (-i\phi_{ij}),$$

$$D = -\frac{3}{2}[(I_{x_i} - iI_{y_i})I_{z_j} + (I_{x_j} - iI_{y_j})I_{z_i}] \sin \theta_{ij} \cos \theta_{ij} \exp (i\phi_{ij}),$$

$$E = -\frac{3}{4} (I_{x_i} + iI_{y_i})(I_{x_j} + iI_{y_j}) \sin^2 \theta_{ij} \exp (-2i\phi_{ij}) , \qquad (4.12)$$

$$F = -\frac{3}{4} (I_{x_i} - iI_{y_i})(I_{x_j} - iI_{y_j}) \sin^2 \theta_{ij} \exp (2i\phi_{ij}) \quad .$$

Terms A and B cannot change total spin in the z-direction and therefore don't contribute to a T_1 measurement. C and D cause total I_z to change by one and E and F by two; so C, D, E and F contribute to T_1.

We define position functions

$$\phi_1(r_{ij}) = \frac{1}{r_{ij}^3} (\sin \theta_{ij} \cos \theta_{ij}) \exp (-i\phi_{ij}) \qquad (4.13)$$

and

$$\phi_2(r_{ij}) = \frac{1}{r_{ij}^3} (\sin^2 \theta_{ij}) \exp (-2i\phi_{ij}) \quad . \qquad (4.14)$$

We calculate the transition rate $1/T_1(\Omega_o)$ from Fermi's Golden Rule. Thus

$$\frac{1}{T_1(\Omega_o)} = \frac{2\pi}{\hbar^2} \sum_G \sum_F |\langle F| \sum_{\substack{i,j \\ i\neq j}} V_{ij}(\underset{\sim}{r}_{12}) |G\rangle|^2 \rho(\omega_f) \delta(\omega_{FG}) \quad . \qquad (4.15)$$

$\hbar\omega_f$ is the two particle energy with no Zeeman field; $\hbar\omega_{FG}$ is the difference in the two particle energy between the final $|F\rangle$ and initial $|G\rangle$ states with a Zeeman field. Physically $T_1(\Omega_o)$ measures the relaxation of the spin system's high temperature to the lower temperature of the lattice. The dipole-dipole interaction allows total spin in the z-direction to be decreased with a consequent decay of the spin temperature. The energy is transferred directly to the molecular and scattering states (considered separately from their spin energy, these states could be said to have a temperature) which are assumed to be tightly coupled to the lattice and thus stay at the lattice temperature.

We first calculate the contribution of term D above. This connects states with m_i to states with m_i-1 where m_i is the z component of the spin of a He^3 atom at site i. We then find the relaxation due to all other He^3 at all other sites j. All sites are equally probable since $kT >> J_{33}$. The result is

$$\frac{1}{T(\Omega_o)_D} = \frac{9}{4}\gamma^4\hbar^2 \sum_j |\langle m_i| [(I_{x_i} - iI_{y_i})I_{z_j} + (I_{x_j} - iI_{y_j})I_{z_i}] |m_i - 1\rangle|^2 j_i(\Omega_o) \qquad (4.16)$$

where, recalling equations 4.13 and 4.14,

$$j_m(\Omega_o) = 2\pi \sum_g \sum_f |\langle f|\phi_m(\underset{\sim}{r}_{12})|g\rangle|^2 \rho(\omega_f)\ \delta(m\Omega_o - \omega_{fg}) \quad . \tag{4.17}$$

$|f\rangle$ and $|g\rangle$ are the spatial parts of the states $|F\rangle$ and $|G\rangle$. Recalling that (35)

$$\langle m_i|I_{x_i} - iI_{y_i}|m_i - 1\rangle = \sqrt{(I+m_i)(I-m_i+1)} \quad , \tag{4.18}$$

we find

$$\frac{1}{T_1(\Omega_o)_D} = \frac{9}{4} x_3 \hbar^2 \gamma^4 m_j^2\ (I+m_i)(I-m_i+1)\ j_1(\Omega_o) \quad , \tag{4.19}$$

Since He^3 has spin $\frac{1}{2}$: $I = \frac{1}{2}$, $m_i = \frac{1}{2}$ and $m_j = \pm\frac{1}{2}$. Then

$$\frac{1}{T_1(\Omega_o)_D} = \frac{9}{16}\ x_3 \hbar^2\ \gamma^4\ j_1(\Omega_o) \quad , \tag{4.20}$$

Similarly for C

$$\frac{1}{T_1(\Omega_o)_C} = \frac{9}{16}\ x_3\ \gamma^4\ \hbar^2\ j_1(\Omega_o) \quad . \tag{4.21}$$

For term F we need to evaluate

$$\frac{1}{T_1(\Omega_o)_F} = \frac{9}{16}\gamma^4\hbar^2 |\langle m_i, m_j|(I_{x_i} - iI_{y_i})(I_{x_j} - iI_{y_j})|m_i - 1, m_j - 1\rangle|^2\ j_2(2\Omega_o) \tag{4.22}$$

$$\frac{1}{T_1(\Omega_o)_F} = \frac{9}{16} x_3 \gamma^4 \hbar^2 j_2(2\Omega_o) \quad . \tag{4.23}$$

Similarly for E

$$\frac{1}{T_1(\Omega_o)_E} = \frac{9}{16} x_3 \gamma^4 \hbar^2 j_2(2\Omega_o) \quad . \tag{4.24}$$

Therefore the total transition rate is

$$\frac{1}{T_1(\Omega_o)} = \frac{9}{8} \hbar^2 \gamma^4 x_3 [j_1(\Omega_o) + j_2(2\Omega_o)] \quad . \tag{4.25}$$

We classify the contributions $j_m(\omega)$ due to the transitions $|g\rangle \rightleftarrows |f\rangle$ as

$$j_m(\omega) = j_m^{(I)}(\omega) + j_m^{(II)}(\omega) + j_m^{(III)}(\omega) \tag{4.26}$$

where the processes are

$$\begin{aligned} &\text{I:} \quad He^3 + He^3 \rightleftarrows He^3 + He^3 \ , \\ &\text{II:} \quad He^3 + He^3 \rightleftarrows (He^3)_2 \ , \\ &\text{III:} \quad (He^3)_2 \rightleftarrows (He^3)_2 \ , \end{aligned} \tag{4.27}$$

Process I is simple scattering. Process II is molecular formation or breakup. Process III represents a transition from one molecular state to another.

The qualitative contributions of these processes can be understood by considering the constraint of energy conservation in the three processes. From figure 12 we expect the effects to be as follows. $j_m^{I}(\omega)$ is centered about $\omega = 0$ with an energy cutoff at $\pm 4zJ_{34}$. $j_m^{II}(\omega)$ is centered about the mean molecular frequency Ω_m with a width of $5zJ_{34}$. $j_m^{III}(\omega)$ is centered about $\omega = 0$ with a cutoff at zJ_{34}.

The strengths of these processes are calculated in Appendix C. We merely quote the results of that analysis here. The strengths of these three processes to second order in (J_{34}/J_{33}) are from equations C.33, C.34 and C.35.

$$F_I^m = \frac{.328\ m^2}{\Delta^6} + \left(\frac{J_{34}}{J_{33}}\right)^2 \frac{2.346\ m^2}{\Delta^6} \quad , \tag{4.28a}$$

$$F_{II}^m = \left(\frac{J_{34}}{J_{33}}\right)^2 \frac{18.724\ m^2}{\Delta^6} \quad , \tag{4.28b}$$

$$F_{III}^m = \frac{1.6\ m^2}{\Delta^6} - \left(\frac{J_{34}}{J_{33}}\right)^2 \frac{39.794\ m^2}{\Delta^6} \quad . \tag{4.28c}$$

We eliminate the angular factors between magnetic field and crystal orientation by power averaging, that is averaging over all crystal orientations relative to the magnetic field direction. From Appendix C the result for $T_1(\Omega_o)$ is then

$$\frac{T_1(0)}{T_1(\Omega_o)} = \frac{j(\Omega_o) + 4j(2\Omega_o)}{5\ j(0)} \quad . \tag{4.29}$$

To fit the experimental results, we used Lorentzian shapes centered at Ω_o and Ω_m with the cutoffs above at three times the Lorentzian width. Thus

$$j(\Omega_o) = \frac{F_I(\Gamma_I/2)^2}{(\Gamma_I/2)^2 + \Omega_o^2} + \frac{F_{II}(\Gamma_{II}/2)^2}{(\Gamma_{II}/2)^2 + (\Omega_o-\Omega_m)^2} + \frac{F_{III}(\Gamma_{III}/2)^2}{(\Gamma_{III}/2)^2 + \Omega_o^2} \tag{4.30}$$

with

$$\Gamma_I = 16J_{34}; \quad \Gamma_{II} = 10J_{34}; \quad \text{and} \quad \Gamma_{III} = 4J_{34} . \tag{4.31}$$

The result is plotted in figure 16 together with the experimental data (36).

Comparison with Experiment and an Alternative Theoretical Model

Since J_{34}/J_{33} was originally thought to be anomalously small in the impuriton gas model, several distortion models were proposed in which long range distortions around defects increased their effective mass and slowed diffusion. We now compare these models with ours and with the experimental data.

The diffusion data have the dependence $D = D_o/x_3^{\alpha}$ (37) where α = 0.8-1.2 in agreement with the impuriton gas model (α = 1). Landesman (38) has calculated α = 4/3 for the distortion model. A similar result has been found using a Monte-Carlo calculation (14). The impuriton gas model is therefore in better agreement with the diffusion data.

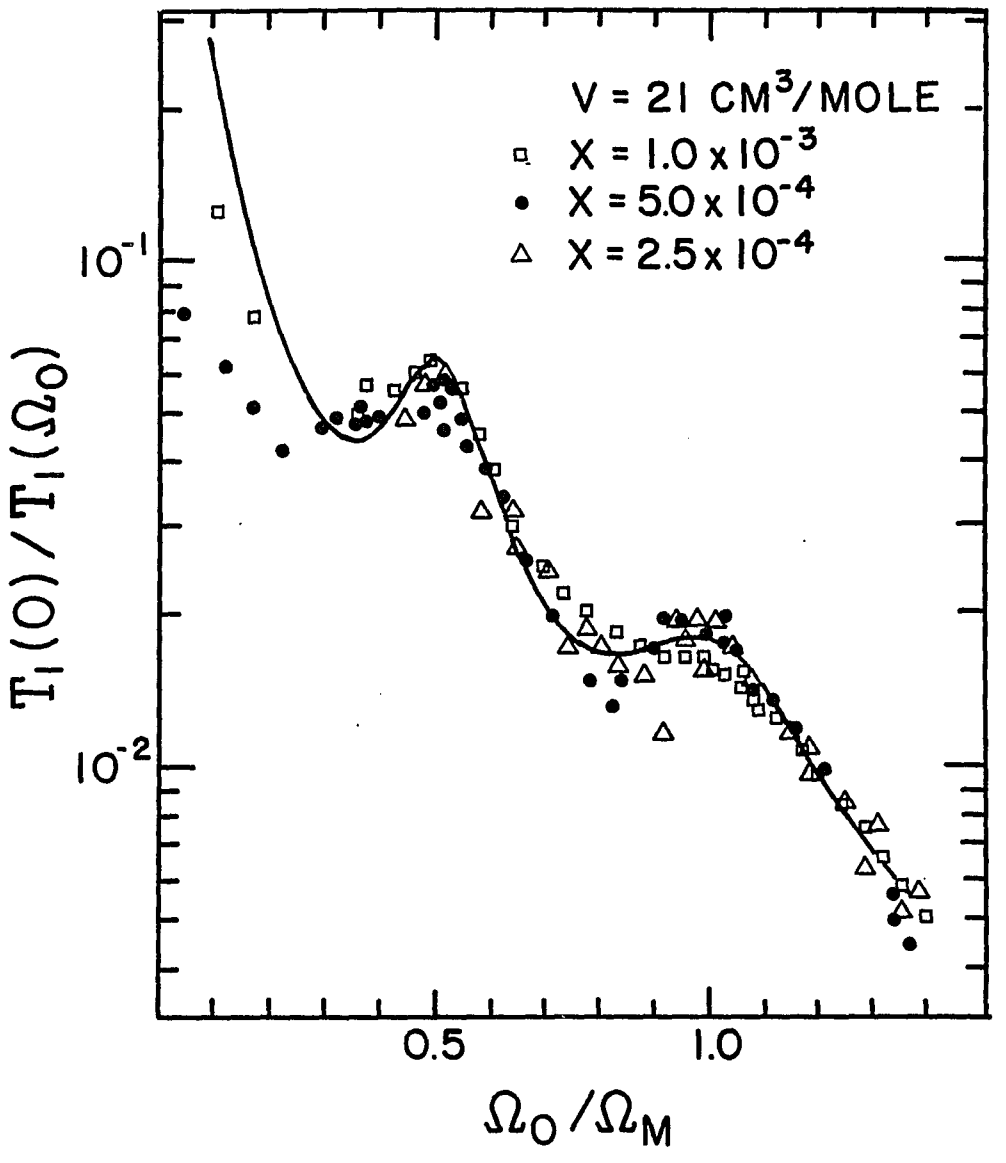

Fig. 16. The inverse of NMR relaxation time of He^3 atoms in solid He^4 as a function of applied magnetic field.

The solid line is the result of the calculation described in the text. The experimental points correspond to the He^3 concentrations given in the figure. The magnetic field dependence is contained in $\Omega_o = \gamma H_o$ and Ω_o has been normalized to Ω_m, the increase of the bound He^3-He^3 triplet molecular energy above the center of the scattering He^3 band (see Fig. 12).

The T_1 data displayed in figure 14 have also been explained using a distortion model in terms of very strongly bound molecules. In the theory of Mullen, Guyer and Goldberg (15), the molecules are constrained to move in A-A or A-B configurations (the HCP lattice is made up of hexagonal planes stacked ABAB...). It is assumed that A-A molecules have elastic energy (V_{AA}) different from that of an AB molecule (V_{AB}) such that $J_{34} << |V_{AA}-V_{AB}|$. Transitions between the two types of molecules then occur at a slow rate. They also assume $kT >> V_{AA}$ so that all states are equally probable which gives $1/T_1 \propto x_3$. They must include both A-B molecules and A-A molecules in the calculation. These make up two molecular bands separated by $|V_{AA}-V_{AB}|$. Presumably B-B molecules contribute in the same way as A-A. They find for $J_{34} = 0.7\ J_{33}$ a double peaked structure roughly like that in figure 16.

The integral $\int_0^\infty \frac{1}{T_1(\omega)}\, d\omega$ is expected to obey a sum rule (36) given by

$$\int_0^\infty \frac{1}{T_1(\omega)}\, d\omega = x_3\, \pi\, M_2 \qquad (4.32)$$

where M_2 is the Van Vleck second moment, which in a HCP crystal is given by (18)

$$M_2 = 22.61 \times 10^{10}/V^2 \qquad (4.33)$$

where V is the molar volume in cm^3/mole. A feature of the theory of Mullen et al. (15) is that 33% of the integral in equation 4.33 is situated in a δ-function around $\omega = 0$. This is in good agreement with

the fact that 50% of the integral is missing from the data (36). This problem is being worked on for the three-dimensional case.

It is clear that both theories have strengths and drawbacks. Further experimental and theoretical work is necessary for a definitive resolution of this problem.

CHAPTER 5

CONCLUSIONS

In this work we have investigated the possibility that bound states along with ground state vacancies play an important role in the description of solid He^4. We have found that for $b/t \gtrsim 3$ (Chapter 2) a vacancy impurity bound state exists in a cubic crystal. It appears likely that this condition is met from other theoretical and experimental work. If one assumes that $b/t \gtrsim 3$ in the BCC phase of solid He^4 and $\lesssim 3$ in its HCP phase, then the existence of these bound states is capable of accounting for the dramatic increase in the diffusion constant (24) as one goes from the HCP to BCC phase. Just why the ratio of b/t should be larger in the BCC phase is not at all obvious. A quantitative calculation of this ratio would be worthwhile but is very difficult.

If such a bound state exists, a more promising and less ambiguous confirmation may be obtained by an alternative experiment. Since the bound state has a hopping frequency which is much greater than J_{34} it makes a significant contribution to the diffusion of He^3 atoms. In the limit of low He^3 concentrations ($x_3 \approx 10^{-3}$-10^{-4}) the diffusion due to these bound states generates a minimum in the He^3 diffusion coefficient as the temperature is raised (figure 7). The experimental

observation of such a minimum at these small concentrations would provide confimation of the existence of this bound state.

The existence of the hopping induced impuriton-impuriton molecule is supported by experimental data although an alternative theory does exist. We have recomputed the He^3 diffusion constant including these bound state effects. We find that the present experimental results are consistent with $J_{33} \sim 10 J_{34}$ rather than the previous (anomalously large) estimate of $J_{33} \sim 10^2\text{-}10^3\ J_{34}$.

In addition, we have fit the $T_1(\Omega)$ data for low concentrations using a theory in which the large J_{33} induces bound states both above and below the free particle band. The transition between triplet states above the band and triplet states within the scattering band lead to two peaks in $T_1(\Omega)$. The two peaks correspond to changes of the z components of spin of $S_z = 1$ and $S_z = 2$. Using a Lorentzian line shape we find excellent agreement between this simple theory and the data.

We have also investigated the possible existence of ground state vacancies from a theoretical point of view. Using a Feynman wave function approach, we have estimated the ground state vacancy concentration at $\approx 10^{-4}$ near melting. This result is most sensitive to our choice of the effective hard sphere radius of He^4 atoms. We here presented evidence that the actual hard sphere radius that should be used is $\sigma \cong$ 3.34 Å rather than $\sigma \cong 2.7$ Å used by Penrose and Onsager (5) to describe liquid helium. This larger value gives the correct peaks in the radial distribution frumction and the correct melting and crystallization volumes. However the condensate fraction in the liquid that we then

predict is $\sim 10^{-5}$ compared to the Penrose and Onsager (5) value of $\sim 10^{-2}$. Contrary to recently published opinion we find that the existence of ground state vacancies is not ruled out by experiment. The theoretical value we obtain for ground state vacancy concentration appears on the contrary to be consistent with experiment.

We find that the vacancy gas will Bose condense at $T_c \sim 10^{-2}$ °K which is not at present experimentally accessible. However, should ground state vacancy concentrations $\approx 10^{-4}$ be present, we would expect the He^3 diffusion constant to be dominated by vacancy-impurity molecules. The experimental results, to date, are unable to give a definitive answer to this possibility. However, should ground state vacancies be present at significant concentrations, then when the temperature becomes comparable to the binding energy ($\sim$ 0.1 °K) of a molecule the diffusion should go up. With impuritons alone it should stay constant as the temperature is decreased.

Finally, we note that the He^4 film on graphite presents an alternative two-dimensional system where many of the above effects may also be present. It is well known (39) that there exist solid phases of such films and that He^3 impurities may be introduced in a controlled way. Thus the calculations we have made may have much broader application than presented here.

APPENDIX A

CALCULATION OF BOUND STATES AND RESONANCES

To solve equation 2.13 it is convenient to use the mixed basis set $|\underset{\sim}{K},\underset{\sim}{R}\rangle$ defined by equation 3.3. In terms of this basis set we can write

$$G_E^{\underset{\sim}{K}',\underset{\sim}{K}}(\underset{\sim}{R}'\underset{\sim}{R}) = \langle \underset{\sim}{K}',\underset{\sim}{R}'|\frac{1}{E-\mathcal{H}_o+i\varepsilon}|\underset{\sim}{K}\ \underset{\sim}{R}\rangle = \delta_{\underset{\sim}{K},\underset{\sim}{K}'}\ G_E^{\underset{\sim}{K}}(\underset{\sim}{R}',\underset{\sim}{R}) \quad . \qquad (A.1)$$

Using equations 3.6 and 3.7 we can write

$$G_E^{\underset{\sim}{K}}(\underset{\sim}{R}',\underset{\sim}{R}) = N^{-1} \sum_{\underset{\sim}{\tau}} \frac{e^{i\underset{\sim}{\tau}\cdot(\underset{\sim}{R}'-\underset{\sim}{R})}}{E-E_{\underset{\sim}{K}}(\underset{\sim}{\tau})+i\varepsilon} \quad , \qquad (A.2)$$

where

$$E_{\underset{\sim}{K}}(\underset{\sim}{\tau}) = -2t \sum_{i=xyz} \cos(\tau_i-\tfrac{1}{2}K_i)\Delta - 2m \sum_{i=xyz} \cos\ (\tau_i+\tfrac{1}{2}K_i)\Delta \qquad (A.3)$$

for a simple cubic lattice with lattice constant Δ. Using the relation

$$(X + i\alpha)^{-1}_{\alpha\to 0^+} = -i \int_o^\infty e^{i(X+i\alpha)\beta}\, d\beta \quad ,$$

we may rewrite equation A.2 as

$$G^{K}_{E}(\underset{\sim}{R}',\underset{\sim}{R}) = \frac{i\Delta^3}{(2\pi)^3}\int_0^\infty d\beta\, e^{i\beta(E-E_{\underset{\sim}{K}}(\tau)+i\varepsilon)}\; e^{i\underset{\sim}{\tau}\cdot(\underset{\sim}{R}'-\underset{\sim}{R})}\, d^3\tau \quad . \qquad (A.4)$$

Since $m \ll t$ ($m \approx 10^{-6}$ t) we can drop the term involving m in the exponent of equation A.4. Equation A.4 may then be written as

$$G^{K}_{E}(\underset{\sim}{R}',\underset{\sim}{R}) = \frac{i\Delta^3}{(2\pi)^3}\int_0^\infty d\beta\, e^{i\beta(E+i\varepsilon)} \prod_{j=1}^{3} I(m_j) \quad , \qquad (A.5)$$

where

$$I(m_j) = \int_{-\pi}^{\pi} \exp\, i[m_j\lambda_j + a\beta\cos\,(\lambda_j+n_j)]\, d\lambda_j \quad , \qquad (A.6)$$

and we have defined $a = 2t$, $\lambda_j = \tau_j\Delta$, $n_j = \frac{1}{2}K_j\Delta$, and $m_j = |\underset{\sim}{R}_j'-\underset{\sim}{R}_j|/\Delta$. In what follows we shall constrain $\underset{\sim}{K}$ to lie on the (1,1,1) axis. Then we may write $n_j = n = K\Delta/2\sqrt{3}$ and

$$I(m_j) = 2\pi\, i^{m_j} J_{m_j}(a\beta)\, e^{-inmj} \qquad (A.7)$$

where J_{m_j} is a Bessel function of the first kind.

As shown by Boyd and Callaway (19), the advantage of using the mixed basis set of equation 2.6 is that the solution to 2.13 may be obtained by considering only the determinant defined by restricting $\underset{\sim}{R}$ and $\underset{\sim}{R}'$ to lie on the origin or the 6 nearest neighbor sites. The truncated matrix for G has elements $G^{K}_{E}(\underset{\sim}{R},\underset{\sim}{R}')$ and is given by

$$
\begin{array}{c|c}
\underset{\sim}{R}' \backslash \underset{\sim}{R} & \begin{array}{ccccccc} 0 & \Delta_x & \Delta_y & \Delta_z & -\Delta_x & -\Delta_y & -\Delta_z \end{array} \\
\begin{array}{c} 0 \\ \Delta_x \\ \Delta_y \\ \Delta_z \\ -\Delta_x \\ -\Delta_y \\ -\Delta_x \end{array} &
\begin{bmatrix}
A_{000} & \alpha^{-1}A_{001} & \alpha^{-1}A_{001} & \alpha^{-1}A_{001} & \alpha A_{001} & \alpha A_{001} & \alpha A_{001} \\
\alpha A_{001} & A_{000} & A_{011} & A_{011} & \alpha^2 A_{002} & \alpha^2 A_{011} & \alpha^2 A_{011} \\
\alpha A_{001} & A_{011} & A_{000} & A_{011} & \alpha^2 A_{011} & \alpha^2 A_{002} & \alpha^2 A_{011} \\
\alpha A_{001} & A_{011} & A_{011} & A_{000} & \alpha^2 A_{011} & \alpha^2 A_{011} & \alpha^2 A_{002} \\
\alpha^{-1}A_{001} & \alpha^{-2}A_{002} & \alpha^{-2}A_{011} & \alpha^{-2}A_{011} & A_{000} & A_{011} & A_{011} \\
\alpha^{-1}A_{001} & \alpha^{-2}A_{011} & \alpha^{-2}A_{002} & \alpha^{-2}A_{011} & A_{011} & A_{000} & A_{011} \\
\alpha^{-1}A_{001} & \alpha^{-2}A_{011} & \alpha^{-2}A_{011} & \alpha^{-2}A_{011} & A_{011} & A_{011} & A_{000}
\end{bmatrix}
\end{array}
\tag{A.8}
$$

where the $A_{jk\ell}$ is defined by equation 3.11, and $\alpha = e^{in}$. This matrix can be nearly diagonalized by use of a matrix

$$
\Gamma = \begin{bmatrix}
1 & 0 & 0 & 0 & 0 & 0 & 0 \\
0 & & & & & & \\
0 & & \gamma & & & \alpha^2\gamma & \\
0 & & & & & & \\
0 & & & & & & \\
0 & & -\alpha^2\gamma & & & \gamma & \\
0 & & & & & &
\end{bmatrix}, \tag{A.9}
$$

where γ is the 3 x 3 matrix given by

$$\Gamma = \begin{bmatrix} 6^{-\frac{1}{2}} & 6^{-\frac{1}{2}} & 6^{-\frac{1}{2}} \\ 12^{-\frac{1}{2}} & 12^{-\frac{1}{2}} & -3^{-\frac{1}{2}} \\ \frac{1}{2} & -\frac{1}{2} & 0 \end{bmatrix} . \qquad \text{(A.10)}$$

The result is

$$\Gamma G \Gamma^{-1} = \begin{bmatrix} A_{000} & 6^{\frac{1}{2}}\alpha^{-1}A_{000} & 0 & 0 & 0 & 0 & 0 \\ 6^{\frac{1}{2}}\alpha A_{001} & A_{000}+A_{002} + 4A_{001} & 0 & 0 & 0 & 0 & 0 \\ 0 & 0 & B & 0 & 0 & 0 & 0 \\ 0 & 0 & 0 & B & 0 & 0 & 0 \\ 0 & 0 & 0 & 0 & C & 0 & 0 \\ 0 & 0 & 0 & 0 & 0 & C & 0 \\ 0 & 0 & 0 & 0 & 0 & 0 & C \end{bmatrix} , \qquad \text{(A.11)}$$

where $B = A_{000} + A_{002} - 2A_{011}$ and $C = A_{000} - A_{002}$.

Using equation 2.8 we find that the only non-zero matrix elements for $\langle \underset{\sim}{K}\ \underset{\sim}{R}|V|\underset{\sim}{K}\ \underset{\sim}{R}' \rangle$ are

$$\langle \underset{\sim}{K}\ \underset{\sim}{0}|V|\underset{\sim}{K} \pm \Delta_j \rangle \quad me^{\pm in} + te^{\mp in}$$

and $\qquad \text{(A.12)}$

$$\langle K\ -\Delta_j|V|K\Delta_j \rangle = -b \quad .$$

Again dropping the terms involving m the matrix for V is

$$\begin{bmatrix} 0 & a\alpha^{-1}/2 & a\alpha^{-1}/2 & a\alpha^{-1}/2 & a\alpha/2 & a\alpha/2 & a\alpha/2 \\ a\alpha/2 & 0 & 0 & 0 & -b & 0 & 0 \\ a\alpha/2 & 0 & 0 & 0 & 0 & -b & 0 \\ a\alpha/2 & 0 & 0 & 0 & 0 & 0 & -b \\ a\alpha^{-1}/2 & -b & 0 & 0 & 0 & 0 & 0 \\ a\alpha^{-1}/2 & 0 & -b & 0 & 0 & 0 & 0 \\ a\alpha^{-1}/2 & 0 & 0 & -b & 0 & 0 & 0 \end{bmatrix}, \tag{A.13}$$

where the same notation as equation A.8 has been used. For the matrix $\Gamma V \Gamma^{-1}$ we have

$$\begin{bmatrix} 0 & 6^{\frac{1}{2}}a\alpha^{-1}/2 & 0 & 0 & 0 & 0 & 0 \\ 6^{\frac{1}{2}}a\alpha/2 & -p & 0 & 0 & q & 0 & 0 \\ 0 & 0 & -p & 0 & 0 & q & 0 \\ 0 & 0 & 0 & -p & 0 & 0 & q \\ 0 & q^* & 0 & 0 & p & 0 & 0 \\ 0 & 0 & q^* & 0 & 0 & p & 0 \\ 0 & 0 & 0 & q^* & 0 & 0 & p \end{bmatrix}. \tag{A.14}$$

where $p = b \cos 2n$ and $q = ib\alpha^2 \sin 2n$.

Finally, the matrix $\Gamma(1-GV)\Gamma^{-1}$

$$\begin{bmatrix} A_{11} & A_{12} & 0 & 0 & A_{15} & 0 & 0 \\ A_{21} & A_{22} & 0 & 0 & A_{25} & 0 & 0 \\ 0 & 0 & A_{33} & 0 & 0 & A_{36} & 0 \\ 0 & 0 & 0 & A_{44} & 0 & 0 & A_{47} \\ 0 & A_{52} & 0 & 0 & A_{55} & 0 & 0 \\ 0 & 0 & A_{63} & 0 & 0 & A_{66} & 0 \\ 0 & 0 & 0 & A_{74} & 0 & 0 & A_{77} \end{bmatrix} , \qquad (A.15)$$

where

$$A_{11} = 1 - 3A_{001} ,$$

$$A_{12} = \frac{-6^{\frac{1}{2}}a}{2\alpha} A_{000} + \frac{6^{\frac{1}{2}}}{\alpha} b A_{001} \cos 2n ,$$

$$A_{21} = \frac{-6^{\frac{1}{2}}a\alpha}{2} (A_{000} + A_{002} + 4A_{001}) ,$$

$$A_{22} = A_{11} + b \cos 2n (A_{000} + A_{002} + 4A_{011}) ,$$

$$A_{15} = -ib\, 6^{\frac{1}{2}} \alpha \sin 2n A_{001} ,$$

$$A_{25} = -ib \alpha^2 \sin 2n (A_{000} + A_{002} + 4A_{011}) ,$$

$$A_{33} = A_{44} = 1 + b \cos 2n (A_{000} + A_{002} - 2A_{011}) ,$$

$$A_{55} = A_{66} = A_{77} = 1 + b \cos 2n (A_{002} - A_{000}) ,$$

$$A_{52} = A_{63} = A_{74} = \frac{-ib}{\alpha^2} \sin 2n (A_{002} - A_{000}) ,$$

$$A_{36} = A_{47} = -ib \alpha^2 \sin 2n (A_{000} + A_{002} - 2A_{011}) ,$$

and the solutions to equation 2.13 are as described in the text.

APPENDIX B

APPLICATIONS OF QUANTUM THEORY OF DIFFUSION TO SOLID He^4

Widom and Richards (40) have shown that the diffusion of defects in solid helium is given by

$$D = \frac{1}{3\hbar^2} \left\langle \left| \frac{\partial E}{\partial \underset{\sim}{K}} \right|^2 \tau_{\underset{\sim}{K}} \right\rangle \tag{B.1}$$

where $\tau_{\underset{\sim}{K}}$ is a collision operator and $\langle\ \rangle$ indicates an average taken with respect to the thermal equilibrium distribution function. In the single collision time approximation this can be written as

$$D = \frac{1}{3} \langle V^2 \rangle \tau_c \tag{B.2}$$

where V is the velocity of the particle.

In what follows we calculate the diffusion of impuritons in a gas of impuritons and then generalize the result to obtain all of the diffusion constants used in Chapter 2. For impuritons the thermal average becomes the average over all states since the bandwidth $2zJ_{34} \ll kT$ where z is the number of nearest neighbors. For the HCP lattice the average of the velocity squared is (22)

$$\langle V^2 \rangle = 18\, J_{34}{}^2\, \Delta^2/\hbar^2 \quad . \tag{B.3}$$

To proceed further we use the techniques of the quantum theory of scattering as applied to solids (20). We define the t matrix for fixed total crystal momentum K as the operator which satisfies

$$V|\psi_{\underset{\sim}{K}}\rangle = t|u_{\underset{\sim}{K}}\rangle \quad . \tag{B.4}$$

$|\psi_{\underset{\sim}{K}}\rangle$ is a state which evolves from the original Bloch state $|u_{\underset{\sim}{K}}\rangle$ through a scattering process which conserves the total crystal momentum $\underset{\sim}{K}$. The Lipmann-Schwinger equation 2.11 may then be written as

$$tu = Vu + VGtu \quad . \tag{B.5}$$

Therefore we have the operator equation

$$t = V + VGt \tag{B.6}$$

with the solution

$$t = V[1 - GV]^{-1} \quad . \tag{B.7}$$

The density of states per site of the crystal per unit energy is given by

$$G(E) = (1/N_s)\ \mathrm{Tr}\ \delta(E-H) \tag{B.8}$$

where Tr means to take the trace and N_s is the number of sites in the crystal. For example, in a crystal with one impurity

$$\begin{aligned} G(E) \rightarrow G_o(E) &= (1/N_s)\ \mathrm{Tr}\ \delta(E-H_o) \\ &= [\Omega/N_s(2\pi)^3] \int d^3K\ \delta[E-E(K)] \quad . \end{aligned} \tag{B.9}$$

Hereafter we shall denote the density of states of a real crystal (containing many impurities) by G(E) whereas $G_o(E)$ will denote the single impurity density of states.

Using the identity for any operator O,

$$\mathrm{Tr}\ [\ell n\ (O)] = \ell n\ [\det\ (O)] \quad , \tag{B.10}$$

which is obvious for O diagonal and thus holds in any representation, and

$$\lim_{\varepsilon \to 0^+} \frac{1}{(x+i\varepsilon)} = P(1/x) - i\pi\ \delta(x) \tag{B.11}$$

where P stands for the principal part, we may rewrite equation B.8 as

$$G(E) = (-1/\pi N_s)\ \mathrm{Im}\ d/dE\ [\ell n\ \det\ (E^+-H)] \tag{B.12}$$

where $E^+ = E+i\varepsilon$. The modification of the density of states due to interaction between impuritons can be isolated by writing

$$E^+-H = (E^+-H_o)\ [1 + (E^+-H_o)^{-1}\ V] \tag{B.13}$$

where H_o is the Hamiltonian for free impurities and V is the impuriton-impuriton interaction. We may now use the fact that det (AB) = det (A) det (B) and

$$G_o(E) = (-1/\pi N_s)\ \mathrm{Im}\ d/dE\ \ell n\ \det\ (E^+ - H_o) \qquad (B.14)$$

to obtain the change in the density of states

$$\Delta N(E) = G(E) - G_o(E) = (-1/\pi N_s)\ \mathrm{Im}\ d/dE\ \{\ell n\ \det[1-(E^+-H_o)^{-1}\ V]\},$$

$$\Delta N(E) = (-1/\pi N_s)\ \mathrm{Im}\ d/dE\ \ell n\ \det\ (1-GV) \qquad (B.15)$$

due to the interaction between impurities.

The det (1-GV) can be written in general as

$$\det\ (1-GV) = \prod_\alpha D_\alpha^{g_\alpha} \qquad (B.16)$$

where D_α are the determinants of the submatrices of 1-GV and g_α is the degeneracy of the α^{th} representation. Then

$$\ell n\ \det\ (1-GV) = \sum_\alpha g_\alpha\ \ell n\ D_\alpha = \sum_\alpha g_\alpha\ [\ell n\ (D_\alpha) - i\delta_\alpha] \quad . \qquad (B.17)$$

δ_α is actually the same phase shift that appears in the usual partial wave expansion. The crucial fact here is that the dimensionality of the matrix V determines the number of phase shifts in the scattering problem. Then

$$\Delta N(E) = (1/\pi N_s) \sum_{\alpha} g_{\alpha} \frac{d\delta_{\alpha}}{dE} \quad . \tag{B.18}$$

For a small concentration x_3 of impuritons only binary collisions are important and equation B.18 becomes

$$\Delta N(E) = \frac{x_3}{\pi} \sum_{\alpha} g_{\alpha} \frac{d\delta_{\alpha}}{dE} = \sum_{\alpha} \Delta N_{\alpha} \quad . \tag{B.19}$$

If we integrate ΔN_{α} over the unperturbed energy band the result must be minus the number of bound states of type α forced out of the band $(-x_3 g_{\alpha} n_{\alpha})$. Then

$$\delta_{\alpha}(E_o) - \delta_{\alpha}(E_m) = \pi n_{\alpha} \tag{B.20}$$

where n_{α} is the number of bound states for the two particle problem in a particular representation α. E_o and E_m are, respectively, the top and the bottom of the unperturbed band. This is analogous to Levinson's theorem in ordinary scattering theory.

We now return to the diffusion problem which from equations B.2 and B.3 has been reduced to a calculation of τ_c. This collision time is given by the optical theorem for the total transition rate as

$$1/\tau_c = (-2x_3/\hbar) \text{ Im Tr} \int \rho(E)\, t(E)\, dE \tag{B.21}$$

where $\rho(E)$ is the two particle density of states. The integral is over the scattering band assuming $J_{34} \ll kT$. The t matrix is related to the phase shift as follows.

$$e^{2i\delta(E)} = 1 - 2\pi\, i\, \rho(E)\, t(E) \tag{B.22}$$

where $\delta(E)$ is the matrix of phase shifts. Therefore

$$1/\tau_c = [2x_3/\hbar\pi\rho(E)] \int \sum_\alpha g_\alpha \sin^2 \delta_\alpha(E)\, \rho(E)\, dE \quad . \tag{B.23}$$

We now approximate $\rho(E)$ with a constant density of states

$$\rho(E) = \frac{1}{4zJ_{34}} \quad . \tag{B.24}$$

Then

$$1/\tau_c = \frac{8zJ_{34}}{\pi} \sum_\alpha g_\alpha \overline{\sin^2 \cdot \delta_\alpha(E)} \tag{B.25}$$

where the bar means to average over all energies in the band. We define

$$\sigma^* = 2 \sum_\alpha g_\alpha \overline{\sin^2 \delta_\alpha(E)} \quad . \tag{B.26}$$

Substituting equations B.3 and B.25 into B.2 we find, using B.26,

$$D = \frac{\pi}{8x_3} \frac{J_{34}a^2}{\hbar\sigma^*} \quad . \tag{B.27}$$

The dimensionality of the matrix V is 26 x 26 due to the two sites per cell and the 12 nearest neighbors in a HCP lattice. However the singlet and triplet parts are 13 x 13 with 12 bound states in either case. Therefore we can take $\sum g_\alpha = 12$ for either triplet or singlet. δ_α goes through $n_\alpha\pi$ between the top and the bottom of the band so we have approximately

$$\overline{\sin^2 \delta_\alpha} \cong 1/2 \qquad \text{(B.28)}$$

for all n_α. Since

$$\sigma^* = 3/4\ \sigma^*_{\text{triplet}} + 1/4\ \sigma^*_{\text{singlet}} \qquad \text{(B.29)}$$

$\sigma^* \cong 12$. This leads to $J_{33} \sim 10 J_{34}$.

Obviously there are a large number of approximations in this result. The physical reason for the difference between the result ($J_{33} \sim 10^2$-$10^3\ J_{34}$) of Richards et al. (2) and this result is the recognition that due to the bound states there is a larger transition rate than with the simple hard core scattering that they assumed. We also note that this result is self consistent in that J_{33} is still large enough to be expected to produce bound states.

The above analysis is easily generalized to obtain the results used in Chapter 2. For impurity vacancy scattering we use $\rho(E) = 1/2zt$, since $t >> J_{34}$, to find (assuming all σ^*'s equal)

$$D_{IV} = \frac{\pi}{4\hbar} \frac{J_{34}^2\ \Delta^2}{X_v t\ \sigma^*} \quad . \qquad \text{(B.30)}$$

For impurity vacancy molecule scattering by vacancies

$$D_{MV} = \frac{\pi}{4\hbar} \frac{(t')^2\ \Delta^2}{X_v (t+t')\ \sigma^*} \quad . \qquad \text{(B.31)}$$

Similarly for scattering of this molecule by impuritons $\rho(E) = \frac{1}{2}zt$ and and $\langle V^2 \rangle = 18\ (t')^2\ \Delta^2$ so

$$D_{MI} = \frac{1}{x_3} \frac{\pi}{4\hbar} \frac{t'\Delta^2}{\sigma^*} \quad . \qquad \text{(B.32)}$$

APPENDIX C

OSCILLATOR STRENGTHS

The oscillator strengths $f_{ab}^{(m)}$ of given processes are given by

$$f_{ab}^{(m)} = \mathrm{Tr}\,\{P_a\,\phi_m\,P_b\,\phi_m\} \tag{C.1}$$

where $\{P_a\}$ are project operators onto the various spatial configurations. We are interested in three types of processes contributing to $j_m(\omega)$ which is related to the oscillator strengths by

$$\int_o^\infty j_m(\omega)\,d\omega = 2\pi \sum_{a,b} f_{ab}^{(m)} \;;\; \sum P_a = 1 \quad . \tag{C.2}$$

We proceed to find the oscillator strengths of each of the three processes: scattering, capture and dissociation, and molecule to molecule scattering.

We write the Hamiltonian in the form

$$H = H_o^{ex} + J_{34}V \tag{C.3}$$

where H_o^{ex} is the He^3-He^3 exchange part and $J_{34}V$, the He^3-He^4 exchange part, is treated as a perturbation. For $J_{34} = 0$ the molecular states are just the nearest neighbor states. Any other state is a dissociated state. We call the projection operators for these molecular states p and use q for the dissociated states. We call the molecular projector

for the real states, with $J_{34} \neq 0$, P and use Q for the real dissociated states. Of course P = 1-Q and p = 1-q. We will only consider the triplet states in the following since the singlet states do not effect T_1.

To find P and Q we use perturbation theory and expand to second order in J_{34} in terms of the unperturbed operators p and q. The result is (41)

$$\begin{aligned} P = p + J_{34}[p\ V(q/c) + (q/c)V\ p] + J_{34}^2\ \{&p\ V(q/c)\ V\ q/c \\ &+ (q/c)\ V\ p\ V(q/c) + (q/c)\ V(q/c)\ V\ p - p\ V\ p(q/c^2) \\ &+ p\ V(q/c^2)\ V\ p - (q/c^2)\ V\ p\ V\ p\} \end{aligned} \tag{C.4}$$

where

$$q/c \equiv q\,\frac{1}{\xi - H_o}\,q = q/\xi \tag{C.5}$$

since $H_o q = 0$. For a triplet molecule $\xi = J_{33}$ where ξ is the energy of the unperturbed triplet molecule so $c = J_{33}$. The result for Q is

$$\begin{aligned} Q = q + J_{34}[q\ V(p/b) + (p/b)\ V\ q] + J_{34}^2\ [&q\ V(p/b)\ V\ (p/b) \\ &+ (p/b)\ V\ q\ V(p/b) + (p/b)\ V(p/b)\ V\ q - q\ V\ q(p/b^2) \\ &- q\ V(p/b^2)\ V\ q - (p/b^2)\ V\ p\ V\ q. \end{aligned}$$

Since $H_o p = J_{33} p$ for the triplet states, $\xi = 0$ for the unperturbed dissociated state, and pp = p, we have

$$p/b = p \frac{1}{\xi - H_o} p = -p/J_{33} \quad . \tag{C.7}$$

For scattering processes the oscillator strength is then

$$\begin{aligned} F_I^{(m)} &= \mathrm{Tr}\,[Q\,\phi_m^*\,Q\,\phi_m] \\ &= \mathrm{Tr}\,[q\,\phi_m^*\,q\,\phi_m] \\ &\quad + \frac{J_{33}}{J_{34}}\,\mathrm{Tr}\,[q\,\phi_m^*\,q\,v\,p\,\phi_m + q\,\phi_m^*\,p\,V\,q\,\phi_m \\ &\qquad + q\,V\,p\,\phi_m^*\,q\,\phi_m + p\,V\,q\,\phi_m^*\,q\,\phi_m] \\ &\quad + \left(\frac{J_{34}}{J_{33}}\right)^2 \mathrm{Tr}\,[-q\,\phi_m^*\,(qVpVq)\,\phi_m - (qVpVq)\,\phi_m^*\,q\,\phi_m \\ &\qquad + q\,V\,p\,\phi_m^*\,p\,V\,q\,\phi_m + p\,V\,q\,\phi_m^*\,q\,V\,p\,\phi_m] \quad . \end{aligned} \tag{C.8}$$

It is evident that the first order terms vanish since none of the terms within the trace connect a state to itself. Using $qq = q$, $pp = p$, the commutative property of the trace and noting that ϕ_m commutes with p and q we find

$$F_I^m = \mathrm{Tr}\,[q|\phi_m|^2 + \left(\frac{J_{34}}{J_{33}}\right)^2 (2\,pVq\,\phi_m^*\,qVp\,\phi_m - 2qVpVq|\phi_m|^2)] \quad . \tag{C.9}$$

Similarly we find for the capture process together with the dissociation process

$$F_{II}^m = 2\,\mathrm{Tr}\,[P\,\phi_m^*\,Q\,\phi_m] \quad . \tag{C.10}$$

Thus

$$F_{II}^{m} = \left(\frac{J_{34}}{J_{33}}\right)^2 \mathrm{Tr}\,[2pVqVp|\phi_m|^2 - 4pVq\,\phi_m^*\,qVp\,\phi_m + 2qVpVq|\phi_m|^2] \quad . \tag{C.11}$$

For the molecule to molecule process

$$\begin{aligned} F_{III}^{m} &= \mathrm{Tr}\,[P\,\phi_m^*\,P\,\phi_m] \\ &= \mathrm{Tr}\,[p|\phi_m|^2] \\ &\quad + \left(\frac{J_{34}}{J_{33}}\right)^2 \mathrm{Tr}\,(2pVq\,\phi_m^*\,qVp\,\phi_m - 2pVqVp|\phi_m|^2) \quad . \end{aligned} \tag{C.12}$$

In NMR calculations one takes the direction of the applied field as the z axis. For a perfect crystalline structure, measurements then depend on the orientation. However, if the sample is a crystalline powder one can average over all orientations. This is the procedure we will follow here since, although solid helium can be produced as a single crystal, no great dependence on orientation has been found.

We first note that

$$\begin{aligned} \phi_1(\underset{\sim}{r}) &= \frac{1}{r^3}\,(\sin\theta\cos\theta)\,e^{-i\phi} \\ &= -\left(\frac{1}{r^3}\right) Y_{21}^*\,\sqrt{8\pi/15} \end{aligned} \tag{C.13}$$

and

$$\phi_2(\underset{\sim}{r}) = \frac{1}{r^3}\sin^2\theta\,e^{-2i\phi} = \frac{1}{r^3}\,Y_{22}^*\,\sqrt{32\pi/15} \quad . \tag{C.14}$$

Therefore we are interested in averaging products of the form $Y_{2m}^{*}(\underset{\sim}{r}_1)\, Y_{2m}(\underset{\sim}{r}_2)$ to get the oscillator strengths to second order. Using the rotation operator

$$R(\alpha,\beta,\gamma) = R_{\gamma}^{x} R_{\beta}^{y} R_{\alpha}^{z} \tag{C.15}$$

where α, β and γ are Euler angles such that

$$\begin{aligned} R_{\alpha}^{z} &= \exp\,(iJ_z\alpha/\hbar) \\ R_{\beta}^{y} &= \exp\,(iJ_y\beta/\hbar) \\ R_{\gamma}^{x} &= \exp\,(iJ_z\gamma/\hbar) \end{aligned} \tag{C.16}$$

and writing $Y_{2m}^{*}(\underset{\sim}{r}_1) = \langle 2m|r_1\rangle$ we find

$$\begin{aligned} Y_{2m}^{*}(\underset{\sim}{r}_1)\, Y_{2m}(\underset{\sim}{r}_2) &= \langle 2m|r_1\rangle\ \langle r_2|2m\rangle \\ &= \langle 2m|R(\alpha\beta\gamma)|r_1\rangle\,\langle r_2|R^{+}(\alpha\beta\gamma)|2m\rangle \\ &= \sum_{u,u'} \langle 2m|R(\alpha\beta\gamma)|2u\rangle\,\langle 2u|r_1\rangle\,\langle r_2|2u'\rangle\,\langle 2u'|R^{+}(\alpha\beta\gamma)|2m\rangle \\ &= \sum_{u,u'} \langle 2u|r_1\rangle\,\langle r_2|2u'\rangle\ D_{mu}^{2}(\alpha\beta\gamma)\, D_{mu'}^{2}(\alpha\beta\gamma) \quad . \end{aligned} \tag{C.17}$$

The D's are Wigner functions (42) with the following orthogonality relationship:

$$\int \frac{d\omega}{8\pi^2} D_{um}^{j}(\alpha\beta\gamma)\, D_{u'm'}^{j'}(\alpha\beta\gamma) = \frac{1}{2j+1}\,\delta_{jj'}\,\delta_{uu'}\,\delta_{mm'} \quad . \tag{C.18}$$

Therefore

$$\int \frac{d\omega}{8\pi^2} Y_{2m}^*(\underset{\sim}{r}_1)\, Y_{2m}(\underset{\sim}{r}_2) = \frac{1}{5} \sum_u Y_{2u}(r_1)\, Y_{2u}(r_2)$$

$$= \frac{1}{4\pi} P_2(\cos\gamma) = \frac{1}{8\pi}(3\cos^2\gamma - 1) \qquad \text{(C.19)}$$

where $\cos\gamma = \dfrac{\underset{\sim}{r}_1 \cdot \underset{\sim}{r}_2}{|\underset{\sim}{r}_1||\underset{\sim}{r}_2|}$ or $\cos\gamma = \underset{\sim}{r}_1 \cdot \underset{\sim}{r}_2$. This result is independent of m so

$$\int \frac{d\omega}{8\pi^2} \phi_1^*(\underset{\sim}{r}_1)\, \phi_1(\underset{\sim}{r}_2) = \frac{(3\cos^2\gamma - 1)}{15\, r_1^3\, r_2^3} \qquad \text{(C.20)}$$

and

$$\int \frac{d\omega}{8\pi^2} \phi_2^*(\underset{\sim}{r}_1)\, \phi_2(\underset{\sim}{r}_2) = 4\,\frac{(3\cos^2\gamma - 1)}{15\, r_1^3\, r_2^3} \quad . \qquad \text{(C.21)}$$

Thus we can evaluate the trace for m = 1 and the values for m = 2 will be four times as great.

To calculate the trace we use the relative coordinate $\underset{\sim}{R} = \underset{\sim}{R}_1 - \underset{\sim}{R}_2$ to define the state $|\underset{\sim}{K},\underset{\sim}{R}\rangle$ previously defined in Appendix A and take the trace with respect to these states. Actually we should use spatially antisymmetric states since only the triplet states contribute to T_1. However V cannot flip $|\underset{\sim}{K},\underset{\sim}{R}\rangle$ into $|\underset{\sim}{K},-\underset{\sim}{R}\rangle$ and the antisymmetric states are linear combinations of the unsymmetrized states. Thus using unsymmetrized states gives a result that is twice as large as that obtained by using antisymmetric states. We account for this factor by taking the trace over only those states with He^3 atom number 1 in the A plane while atom number 2 takes any other location. The other states would be expected to give an equal contribution to these.

We now evaluate the terms in the strengths. For the zero order terms $\gamma = 0$. Thus

$$\text{Tr } q|\phi_m|^2 = \frac{m^2}{15} \sum_{r_i>a} \frac{3\cos^2\gamma - 1}{r^6} = \frac{.328\ m^2}{\Delta^6} \qquad \text{(C.22)}$$

and

$$\text{Tr } p|\phi_m|^2 = \frac{m^2}{15} \sum_{r_1=a} \frac{3\cos^2\gamma - 1}{r^6} = \frac{1.6\ m^2}{\Delta^6} \quad . \qquad \text{(C.23)}$$

The first second order term we will consider is $\text{Tr}(pVqVp|\phi_m|^2)$. Clearly $\gamma = 0$ for any contribution to this term. Thus we simply need to calculate the number of ways the molecule can break up and then return to its original state. By studying the HCP lattice we see that there are 12 possible orientations (N_O) of a molecule with atom 1 in the A plane and 14 possible ways (N_w) for either end to move and break up the state. Therefore

$$\text{Tr } (pVqVp|\phi_m|^2) = \frac{m^2}{15} \frac{3\cos^2\gamma - 1}{\Delta^6} N_O N_w = \frac{22.4}{\Delta^6} . \qquad \text{(C.24)}$$

The calculation of the Tr $(pVq\ \phi_m^*\ qVp\ \phi_m)$ is more difficult since we have different γ's for different types of molecular breakups. We first consider breakups where the molecule stays in the A plane. Suppose the molecule is oriented along the basis vector $a_2 = (0,\Delta,0)$. There are three places atom 2 can hop to, labeled a, b and c in figure 17. The three corresponding dissociated state vectors are (recalling that the basis vector $a_1 = \Delta(\sqrt{3}/2, -\frac{1}{2}, 0)$:

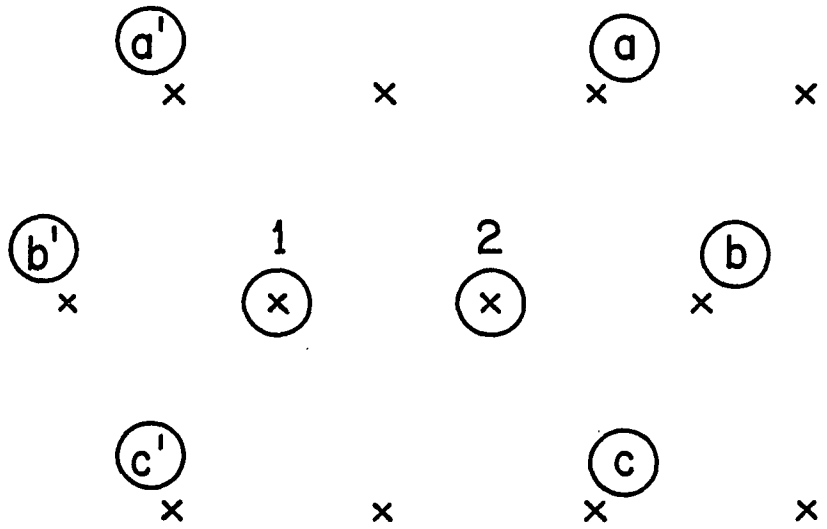

Fig. 17. Possible molecular breakups in the A-plane.

Atom 2 can hop to positions a, b or c causing a molecular breakup in the A-plane. Atom 1 has a similar set of hops a', b' and c'. Hops to the B-plane are considered as a separate contribution in the text.

$$\begin{aligned} \underset{\sim}{r}_1 &= \underset{\sim}{a}_2 - \underset{\sim}{a}_1 = \Delta\sqrt{3}(-\tfrac{1}{2}, \sqrt{3}/2, 0) \quad , \\ \underset{\sim}{r}_2 &= 2\underset{\sim}{a}_2 = 2\Delta(0,1,0) \quad , \\ \underset{\sim}{r}_3 &= 2\underset{\sim}{a}_2 + \underset{\sim}{a}_1 = \Delta\sqrt{3}(\tfrac{1}{2}, \sqrt{3}/2, 0) \quad . \end{aligned} \tag{C.25}$$

Using $\cos(\gamma_1) = \cos(\gamma_3) = \sqrt{3}/2$ and $\cos(\gamma_2) = 1$ along with $|\underset{\sim}{r}_1| = |\underset{\sim}{r}_3| = \sqrt{3}\Delta$ and $|\underset{\sim}{r}_2| = \Delta\sqrt{2}$ we find, calling this contribution A_1, with $N_0 = 6$:

$$\begin{aligned} A_1 &= \frac{2N_0 m^2}{15}\left[\frac{2(3\cos^2\gamma_1 - 1)}{r_1^3\,\Delta^3} + \frac{3\cos^2\gamma_2 - 1}{r_2^3\,\Delta^3}\right] \\ &= \frac{.5849\ m^2}{\Delta^6} \quad . \end{aligned} \tag{C.26}$$

There is a factor of two in all these results since, if atom 1 hops, identical contributions to those produced by atom 2 hopping are produced.

Next we calculate the contribution for jumps from AA to AB and back to the original AA molecule where, for example, AA means that both atoms are in the A plane. The vector $b = \Delta(\sqrt{1/3}, 0, \sqrt{2/3})$ connects A and B planes. Recalling that the basis vector $\underset{\sim}{a}_3 = \Delta(0,0,\sqrt{8/3})$, the four dissociated orientations produced by atom 2 hopping with the molecule initially oriented along $\underset{\sim}{a}_2$ are

$$\begin{aligned} \underset{\sim}{r}_1 &= \underset{\sim}{a}_2 - \underset{\sim}{a}_1 + \underset{\sim}{b} = \Delta\sqrt{3}(-1/6, \sqrt{3}/2, \sqrt{2}/3) \\ \underset{\sim}{r}_2 &= \underset{\sim}{r}_1 - \underset{\sim}{a}_3 = \Delta\sqrt{3}(-1/6, \sqrt{3}/2, -\sqrt{2}/3) \end{aligned} \tag{C.27}$$

$$\begin{aligned} \underset{\sim}{r}_3 &= \underset{\sim}{a}_2+\underset{\sim}{b} = \Delta\sqrt{2}(\sqrt{1/6},\sqrt{1/2},\sqrt{1/3}) \\ \underset{\sim}{r}_4 &= \underset{\sim}{a}_2-\underset{\sim}{a}_3+\underset{\sim}{b} = \Delta\sqrt{2}(\sqrt{1/6},\sqrt{1/2},-\sqrt{1/3}) \quad . \end{aligned} \tag{C.27}$$

These four vectors reduce to two types: two $(\underset{\sim}{r}_1,\underset{\sim}{r}_2)$ with cos $(\gamma_1) = 3/2$ and $|\underset{\sim}{r}_1| = \Delta\sqrt{3}$ and two $(\underset{\sim}{r}_3,\underset{\sim}{r}_4)$ with cos $(\gamma_2) = 1/2$ and $|r_2| = \Delta\sqrt{2}$. This contribution (A_2) is then, with $N_0 = 6$:

$$A_2 = \frac{8N_0m^2}{15}\left[\frac{3\cos^2\gamma_1 - 1}{r_1^3\Delta^3} + \frac{3\cos^2\gamma_2 - 1}{r_2^3\Delta^3}\right] = \frac{.6677\ m^2}{\Delta^6} . \tag{C.28}$$

There is another contribution (A_3) from dissociations of AB molecules. We take the orientation along B. The seven orientations produced by one end hopping are

$$\begin{aligned} \underset{\sim}{r}_1 &= \underset{\sim}{a}_3 = \Delta\sqrt{8/3}(0,0,1) \\ \underset{\sim}{r}_2 &= \underset{\sim}{a}_1+\underset{\sim}{a}_3 = \Delta\sqrt{11/3}(3/2\sqrt{11},-\tfrac{1}{2}\sqrt{3/11},\sqrt{8/11}) \\ \underset{\sim}{r}_3 &= \underset{\sim}{a}_1+\underset{\sim}{a}_2+\underset{\sim}{a}_3 = \Delta\sqrt{11/3}(3/2\sqrt{11},\sqrt{3/11},\sqrt{8/11}) \\ \underset{\sim}{r}_4 &= \underset{\sim}{b}+\underset{\sim}{a}_2 = \Delta\sqrt{2}(\sqrt{1/6},\sqrt{1/2},\sqrt{1/3}) \\ \underset{\sim}{r}_5 &= \underset{\sim}{b}-\underset{\sim}{a}_2 = \Delta\sqrt{2}(\sqrt{1/6},-\sqrt{1/2},\sqrt{1/3}) \\ \underset{\sim}{r}_6 &= \underset{\sim}{b}+\underset{\sim}{a}_2+\underset{\sim}{a}_1 = \Delta\sqrt{3}(5/6,\tfrac{1}{2}\sqrt{3},\sqrt{2}/3) \\ \underset{\sim}{r}_7 &= \underset{\sim}{b}+\underset{\sim}{a}_1 = \Delta\sqrt{3}(5/6,-\tfrac{1}{2}\sqrt{3},\sqrt{2}/3) \quad . \end{aligned} \tag{C.29}$$

These are of four types: one $(\underset{\sim}{r}_1)$ with cos $(\gamma_1) = \sqrt{2/3}$ and $|r_1| = \Delta\sqrt{8/3}$, two $(\underset{\sim}{r}_2,\underset{\sim}{r}_3)$ with cos $(\gamma_2) = \sqrt{11/12}$ and $|r_2| = \Delta\sqrt{11/3}$,

two ($\underset{\sim}{r}_4, \underset{\sim}{r}_5$) with cos ($\gamma_3$) = $\sqrt{1/2}$ and $|\underset{\sim}{r}_3| = \Delta\sqrt{2}$, and two ($\underset{\sim}{r}_6, \underset{\sim}{r}_7$) with cos ($\gamma_4$) = $\sqrt{3/2}$ and $|\underset{\sim}{r}_4| = \Delta\sqrt{3}$. Thus

$$A_3 = \frac{2N_0 m^2}{15}\left[\frac{3\cos^2\gamma_1 - 1}{r_1^3\,\Delta^3} + \frac{2(3\cos^2\gamma_2 - 1)}{r_2^3\,\Delta^3}\right.$$

$$\left. + \frac{2(3\cos^2\gamma_3 - 1)}{r_3^3\,\Delta^3} + \frac{2(3\cos^2\gamma_4 - 1)}{r_4^3\,\Delta^3}\right] \qquad (C.30)$$

$$A_3 = \frac{.5825\ m^2}{\Delta^6} \quad .$$

Hence

$$\text{Tr}\ (pVq\ \phi_m^*\ qVp\ \phi_m) = A_1 + A_2 + A_3 = \frac{1.835\ m^2}{\Delta^6} \quad . \qquad (C.31)$$

The last term needed is Tr ($qVpVq|\phi_m|^2$). In this case, for all contributions, cos (γ_i) = 1. Thus we simply replace all cos (γ_i) in equations C.26, C.28 and C.30 by one and add the three contributions to find,

$$\text{Tr}\ (qVpVq|\phi_m|^2) = \frac{1.330\ m^2}{\Delta^6} \quad ,$$

where all $r_i^3\,\Delta^3$ are replaced by r_i^6 since $|\phi_m|^2$ operates on the dissociated state.

We can now evaluate the oscillator strengths for the various processes by substituting equations C.22, C.23, C.24, C.31 and C.32 into equations C.9, C.11 and C.12. Thus,

$$F_I^m = \frac{.328\ m^2}{\Delta^6} + \left(\frac{J_{34}}{J_{33}}\right)^2 \frac{2.346\ m^2}{\Delta^6} \quad , \tag{C.33}$$

$$F_{II}^m = \left(\frac{J_{34}}{J_{33}}\right)^2 \frac{18.724\ m^2}{\Delta^6} \quad , \tag{C.34}$$

$$F_{III}^m = \frac{1.6\ m^2}{\Delta^6} - \left(\frac{J_{34}}{J_{33}}\right)^2 \frac{39.794\ m^2}{\Delta^6} \quad . \tag{C.35}$$

REFERENCES

1. Andreev, A. F., and I. M. Lifshitz, Zh. Eksp. Teor. Fiz. 56, 2057 (1969) [English transl., Soviet Phys.-JETP 29, 1107 (1969).

2. Richards, M. G., J. Pope, and A. Widom, Phys. Rev. Lett. 29, 708 (1972).

3. Locke, Douglas P., and Richard A. Young, J. Low Temp. Phys. 23, 177 (1976).

4. Miyoshi, D. S., R. M. Cotts, A. S. Greenberg, and R. C. Richardson, Phys. Rev. A 2, 870 (1970).

5. Penrose, O., and L. Onsager, Phys. Rev. 104, 576 (1956).

6. Chester, G. V., Phys. Rev. A 2, 256 (1970).

7. Widom, A., and J. B. Sokoloff, J. Low Temp. Phys. 21, 463 (1975).

8. Greywall, D. S., Phys. Rev. B 11, 4717 (1975).

9. Leggett, A. J., Phys. Rev. Lett. 25, 1543 (1970).

10. Guyer, R. A., Phys. Rev. Lett. 26, 174 (1971).

11. Londesman, A., and J. M. Winter, Low Temperature Physics, ed. by W. J. O'Sullivan, K. D. Timmerhaus and E. F. Hammel. (Plenum, New York, 1973), Vol. 2, p. 73.

12. Huan, W., H. A. Goldberg, and R. A. Guyer, Phys. Rev. B 11, 3384 (1975).

13. Yamashita, Y., J. Phys. Soc. Japan 37, 1210 (1974).

14. Takemore, M. T., and R. A. Guyer, Phys. Rev. Lett. 33, 283 (1974).

15. Mullin, W. J., R. A. Guyer, and H. A. Goldberg, Phys. Rev. Lett. 35, 1007 (1975).

16. Mineev, V. P., Zh. Eksp. Teor. Fiz. 63, 1822 (1972) [English transl., Soviet Physics-JETP 36, 964 (1973)].

17. Guyer, R. A., J. Low Temp. Phys. 8, 427 (1972).

18. Guyer, R. A., R. C. Richardson, and L. I. Zane, Rev. Mod. Phys. 43, 532 (1971).

19. Boyd, R. G., and J. Callaway, Phys. Rev. 138, A1621 (1965).

20. Callaway, J., Quantum Theory of the Solid State. (Academic Press, New York, 1974), Chapter 5.

21. Wolfram, T., and J. Callaway, Phys. Rev. 130, 2207 (1963).

22. Sacco, J. E., and A. Widom, J. Low Temp. Phys. (in press, 1976).

23. Grigoriev, V. N., B. N. Eselson, V. A. Mikheev, V. A. Slusarev, M. A. Strzhemechny, and Y. N. Shulman, J. Low Temp. Phys. 13(1/2), 65 (1973).

24. Grigoriev, V. N., B. N. Eselson, and V. A. Mikheev, Sov. J. Low Temp. Phys. 1, 1 (1975).

25. Reich, H. A., Phys. Rev. 129, 630 (1963).

26. Woo, Chai-Wei, "Microscopic Calculations for Condensed Phases of Helium," in Physics of Liquid and Solid Helium, ed. by K. H. Benneman and J. B. Ketterson. (John Wiley Interscience, in press, 1976).

27. Bernal, J. D., and S. V. King, "Experimental Studies of a Simple Liquid Model," in Physics of Simple Liquids, ed. by N. V. Temperley, J. S. Rowlinson, and G. S. Rushbrooke. (North-Holland Publ. Co., Amsterdam, 1968), Chapter 6.

28. de Llano, M., and S. Ramirez, J. Chem. Phys. 62, 4242 (1975).

29. Wilks, John, The Properties of Liquid and Solid Helium. (Clarendon Press, Oxford, 1967), p. 579.

30. Salzburg, Z. W., W. G. Rudd, and F. H. Stillinger, J. Chem. Phys. 47, 4534 (1967).

31. Hoover, W. G., and F. H. Ree, J. Chem. Phys. 49, 3609 (1968).

32. Widom, A., and D. P. Locke, J. Low Temp. Phys. 23, 335 (1976).

33. Sacco, J. E., A. Widom, D. P. Locke, and M. G. Richards, Phys. Rev. Lett. 37, 760 (1976).

34. Andrew, E. R., Nuclear Magnetic Resonance. (Cambridge University Press, New York, 1958), Appendix 3.

35. Condon, E. U., and G. H. Shortley, The Theory of Atomic Spectra. (Cambridge University Press, New York, 1935), Chapter 3.

36. Richards, M. G., J. H. Smith, P. S. Tofts, and W. J. Mullin, Phys. Rev. Lett. 34, 1545 (1975).

37. Richards, M. G., J. Pope, and A. Widom, "NMR Measurements on ^{3}He Impurities in Solid ^{4}He," in Low Temperature Physics LT-13, Vol. 2, p. 67 (1974).

38. Landesman, A., Phys. Lett. 54A, 137 (1975).

39. Dash, J. G., Films on Solid Surfaces. (Academic Press, New York, 1975), Chapter 7.

40. Widom, A., and M. G. Richards, Phys. Rev. A 6, 1196 (1972).

41. Messiah, Albert, Quantum Mechanics. (John Wiley & Sons, Inc., New York, 1962), Vol. II, Chapter 16.

42. Davydov, A. S., Quantum Mechanics. (NEO Press, Ann Arbor, 1966), Chapter 6.